Towards a Stable Three-Legged Under-Actuated Robotic Platform

Jacob Daniel Webb

Thesis submitted to the faculty of the Virginia Polytechnic Institute and State University in partial fulfillment of the requirements for the degree of

Master of Science
In
Mechanical Engineering

Dennis Hong
Alexander Leonessa
Bob Sturges

December 8th 2014
Blacksburg, VA

Keywords: robot, robotics, under-actuated, tall, three, legged, thaler, strider

Towards a Stable Three-Legged Under-Actuated Robotic Platform

Jacob Daniel Webb

ABSTRACT

The work seeks toward further developing a novel robotic platform capable of stable three legged locomotion. This will be accomplished by creating a robust and adaptable robotic platform capable of executing different walking strategies and taking multiple continuous steps. Previous iterations of this platform have been developed, all of which have used a single gait strategy. This study will seek to develop two new strategies. The first of which is a modification of the original strategy with theoretically improved gate robustness. A second strategy will seek to implement more advanced control techniques to create a fully stable balanced gait.

TABLE OF CONTENTS

LIST OF FIGURES

LIST OF TABLES

1 BACKGROUND

The Tri-Pedal, Hyper, Altitudinal, Legged, Robot (THALeR) Platform is a three legged robot with 12 actuated degrees of freedom. The feet of the system are un-actuated. The approximate geometry of the platform is shown below in figure 1.

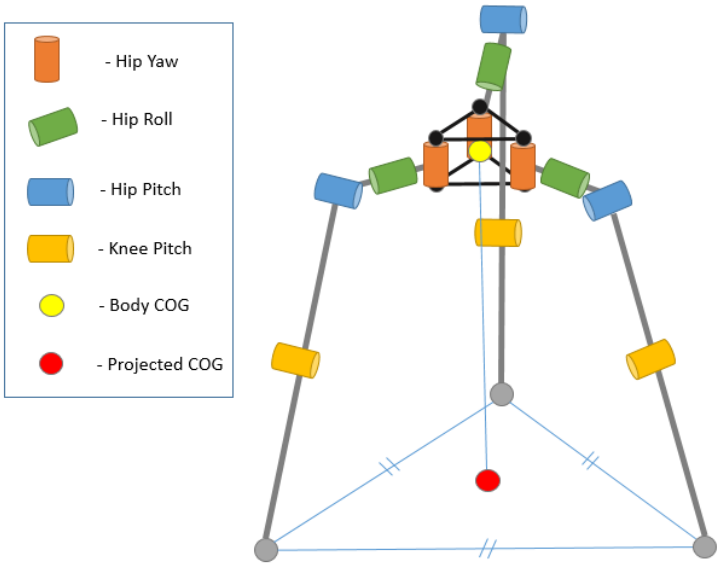

Figure 1 – Geometric Layout of THALeR Platform in Equilateral Stance

The platform has been in development for a number of years and has undergone multiple revisions each gradually increasing in height [1-7].

1.1 PRACTICAL MOTIVATION

DARPA funded the THALeR Project with the long term goal of developing a very tall (30 foot) robotic platform. This could potentially serve as a mobile communications or surveillance system capable of walking along with troops or navigating itself in hostile territory.

Fundamentally it is a project to study how the height of a robotic platform effects mobility. Any legged robotic platform when faced with an obstacle that is too high to step over must find a way to navigate around the obstacle at the expense of time and computation complexity. However, in theory if one drastically increases the height of said platform, obstacles that would previously have to be navigated around can now simply be stepped over. THALeR is designed to explore the feasibility of designing a robot capable of traversing obstacles in such a manner.

1.2 SCIENTIFIC MOTIVATION

The research motivation towards developing the THALeR platform focuses on creating a minimalistic tri-pedal platform that uses a novel gait. The three legged configuration was chosen in order to provide a statically stable stance using the fewest actuators possible for the lowest power consumption and minimal control effort (no active balancing). [1-7]

The three legged configuration does however come at the expense of increased walking difficulty. Since each ankle is unactuated as soon as the robot lifts one leg it is inherently unstable and immediately starts to fall over. This means the system needs to catch itself from falling while trying to complete a successful step. This dynamic walk is another fundamental scientific motivation for the project. Most legged robots are always balancing even while lifting one foot to complete a step. This is usually possible with either actuated ankles or more legs for extra support. THALeR however has neither of these features and thereforee must implement a very unique walking strategy, the "swing through" step, detailed below in figure 2. [1-7]

The platform completes a "swing through" step by aligning the hip roll joints of two legs ("stance legs") to act as an axis about which the rest of the robot pivots (figure 3). The third leg, the "swing leg", pushes off the ground and leaves contact turning the system into a large inverted pendulum. The swing leg and entire body then pass between the fixed stance legs while rotating about the aligned hip roll axis. The swing leg and body then reorient themselves in order to place the swing foot in the desired location before the entire system falls. The development of this dynamic walk is another primary scientific motivation for the THALeR Project. [1-7]

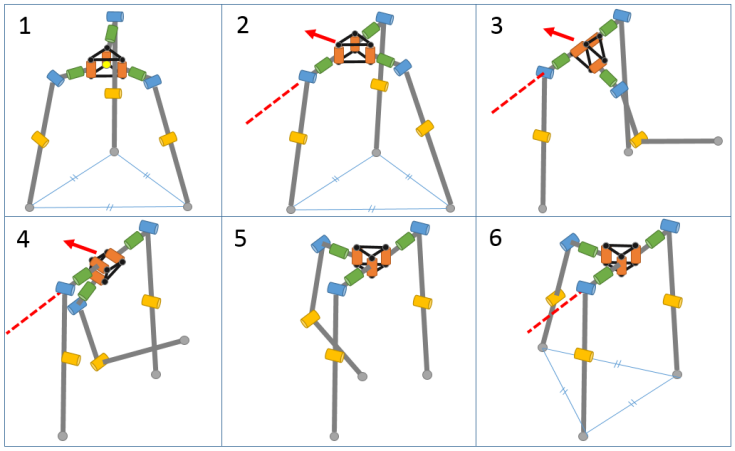

Figure 2 – Overview of "Swing Through" Gait Strategy

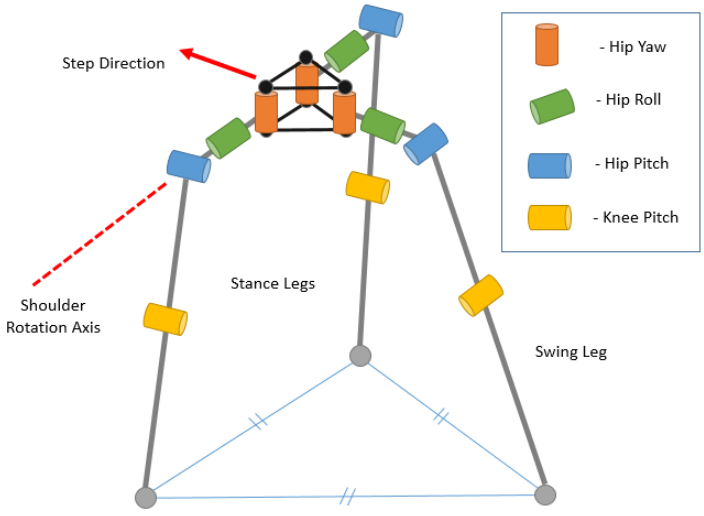

Figure 3 – Adjusted platform geometry, "Ready to Step" state

The platform completes multiple steps by walking in a zig-zag pattern detailed below in figure 4.[1-7] If one assigns constant letter designations to each foot of the platform (A,B,C) we can track the position of each foot as the robot traverses a path.

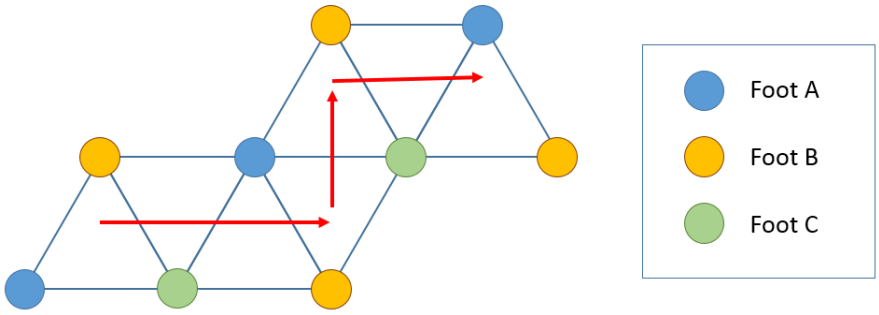

Figure 4 – Multiple step walking pattern

1.3 PREVIOUS PLATFORM REVISIONS

The THALeR platform has gone through three revisions since 2006. [1-7] Two versions fell under the STriDER (Self Excited Tri-Pedal Dynamic Experimental Robot) project and a third was a 9 Degree of Freedom (DOF) test platform for the THALeR. Each platform gradually increased in height and attempted to produce a repeatable gait. All previous robots produced a single step that was non-repeatable. [1-7] This study seeks to produce a platform that can complete a single repeatable as well as successive repeatable steps.

2 MECHANICAL DESIGN

The overall goal of the THALeR Program is to build a 10 meter tall three legged robotic platform. The present goal is to use a specific set of prototype rotary servo actuators to create a system that is as tall as possible. The mechanical design process will start with the selection of all the components necessary for the system to function.

2.1 COMPONENTS

2.1.1 ACTUATORS

The actuators used throughout the system are off-the-shelf servo actuators from Robotis that communicate via daisy-chained RS232 serial connection at one mega baud. The actuators come in three form factors with respective power ratings. The motor details are as follows;

Table 1 – Dynamixel PRO Sizes and Specifications

Power	Voltage (V)	Cont. Torque (Nm)	Cont. Speed (rpm)	Weight (g)
20W	24	5.6	15.6	340
100W	24	21.1	32.7	732
200W	24	39.2	32.1	855

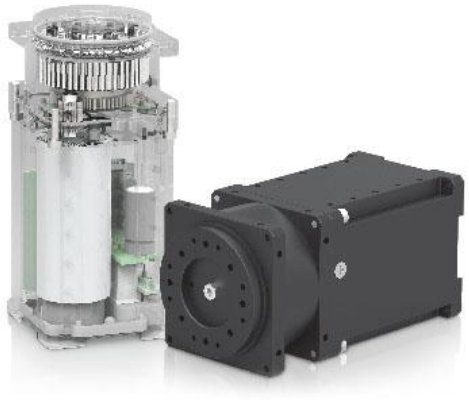

Figure 5 - Dynamixel PRO Actuator (100W)
www.robotshop.com used under fair use 2014

The actuators include built-in motor drivers capable of commanding the motor in position, velocity, or torque mode. For the purposes of this study we will be operating the motors in position mode.

2.1.2 INERTIAL MEASUREMENT UNIT (IMU)

The feet of the robotic platform are unactuated and unsensed. Thereforee in order to determine the orientation of the platform with the ground an inertial measurement unit will be used. For this purpose a Microstrain 3DM-GX4-45 was chosen.

The data output rate is up to 500 Hz with an angle accuracy of $\pm 0.25°$ in roll and pitch and $\pm 0.8°$ in yaw.

Figure 6 – Microstrain IMU 3DM-GX4-45
www.microstrain.com used under air use 2014

2.1.3 COMPUTER

The basic requirements of the onboard computer are to take a previously planned time-based joint-space trajectory and forward the position commands to the motors themselves. In addition the data from the IMU needs to be read into whatever control system will be used. The lab uses a standard software framework across all our platforms that is Linux based, therefore the computer should be Linux capable. In order to interface with the actuators and IMU two USB ports are needed. In addition the computer should be WiFi enabled in order to allow wireless communication. Finally the computer should be as small, light-weight, and energy efficient. With all of these factors in mind a Fit-PC2 was chosen for the onboard computer. The FitPC2 features a 1.6Ghz Intel Atom processor and 2mb of ram. In addition the PC features all of the ports and communication protocols necessary to connect with peripherals.

Figure 7 – Fit PC2 Computer
www.fit-pc.com used under air use 2014

2.1.4 BATTERIES

Ideally the entire system should be power independent. However increased battery capacity comes at the expense of increased weight. We would like to have enough untethered run time enough for a live demonstration between 15 to 30 minutes.

The lab had access to a 6 degree of freedom arm made entirely of the same motors of varying sizes. We used this arm to estimate the power draw of the combimed system of actuators. During operation the average current draw was approximately 6 amps. There with 12 actuators and an average current draw of 1 amp per actuator, a 4000 mAh battery should give approximately 20 mins of runtime. With this in mind a 2 cell, 7.4V, 4000mAh battery was sourced from MaxAmps.com. Three of these batteries, when wired in series, would provide 22.2 Volts nominally.

Figure 8 – MaxAmps Battery
www.maxamps.com used under fair use 2014

2.1.5 SLIP RING

Inclusion of a slip ring at the hip roll joint enables the platform to walk in a single direction without the cables wrapping around the body as it rotates between the stance legs. The slip ring must carry all of the power necessary to drive both the hip and knee pitch actuators as well as the serial data for actuator communication. The miniature slip rings provided by Moog came in a number of different models where the main difference is package size and the number of separate wires.

Figure 9 – Moog Slip Ring SRA-73683
www.moog.com used under fair use 2014

Each wire is capable of carrying a maximum of one amp. Since the serial connection requires four wires itself, a 24 wire slip ring will allow 10 wires each for the positive and ground power connections for the motor. Therefore allowing 10 amps of throughput. At 24 Volts this allows 240 Watts of power which should be more than sufficient to power two 100 Watt actuators but nothing more. The 24 wire version of the chosen slip rings were the largest wire bundle available in that model. Since that model was also the only one of the appropriate size to fit in any reasonably sized assembly it was decided to use 100 Watt motors in both the knee and hip pitch joints of the robot to meet the power limitations of the slip ring.

2.1.6 CARBON FIBER TUBES

The final component to consider in the design are the carbon fiber tubes that will make up the majority of the legs for the system. Carbon fiber was chosen for its weight and strength characteristics, but also for its extremely high flexibility. One of the largest concerns for the platform based on testing of previous robot models was impact loading on the gear-train of the actuators when the swing foot impacts the ground. In the past this impact led to frequent damaging of actuators and structural components. These previous actuators were relatively inexpensive and therefore relatively affordable to replace. However, the

Dynamixel PRO motors cost in the thousands of dollars and we therefore wished to extend the life of them as long as possible by minimizing the impact force on the actuators. Numerous different methods were investigated but in the end one of the simplest was chosen whereby one could greatly reduce impact forces by allowing compliance in the legs themselves. This was done by sourcing 0.75 diameter hollow carbon fiber tubes and using them as the primary structure of both the upper and lower legs. This size was chosen based on testing of multiple different sizes of tubes from the same manufacturer to find a size that offered suitable structural rigidity while still allowing compliance on impact. It was also decided early on to make the leg assembly modular in case the selected size of carbon tube needed to be modified. With modularity the carbon fiber tubes could be switched out quickly and easily.

2.2 JOINT ACTUATOR SIZING

The next step in the mechanical design is to take what we currently know about the system and its components and choose the appropriate motor size to suite the joint requirements. The original goal of the project was to use the provided actuators to build the tallest robot possible. However, given the fact that all further calculations to determine appropriate actuator size rely on choosing a robot height first it was decided to attempt to make the robot as tall as could actually fit in the lab's testing area. With this assumption we can proceed to determine if there was a feasible arrangement of actuators that could support such a structure. If not then we would decrease the assumed height of the system and repeat the analysis.

To start the actuator sizing analysis we will assume the system is in an "equilateral stance" (figure 10). We will also assume the robot's overall height is one foot shorter than the ceiling height of the testing area which happens to be almost exactly 3 meters high (10 ft). This is the tallest the system can be and still be able to test it in the labs available space. In addition we must define the geometry of the equilateral stance to proceed with calculations. The equilateral stance is defined as having each foot at the corner of an equilateral triangle mapped onto the ground plane. The knee joints are straight and each hip joint points from the center of the body straight out towards each foot (figure 10).

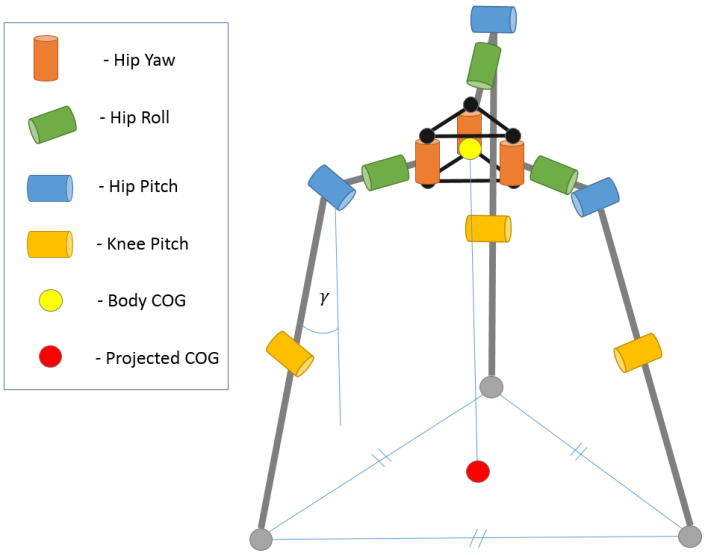

Figure 10 – Equilateral Stance

In this pose we will assume that the standard angle of each hip pitch joint is 10 degrees with the vertical and will be designated as "γ". In addition we must define a distance from the body center of gravity (COG) to the hip pitch axis. We will define this as the "hip span" and estimate it to be as long as

realistically possible as a worst case scenario. Making the hip span longer implies increasing the moment arm on the hip yaw joint while taking a step and it also increases the moment arm on the hip pitch axis both while standing and stepping. The worst case length for the hip span will be estimated by assuming the hip roll actuator is the longest of the three motor types (200W) and the moog slip ring will be placed directly in-line with the motor ahead of the motor horn (figure 11). Finally we will assume the width of the hip pitch actuator matches the width of the widest motor type (200W or 100W). We can also add a factor of safety for wires and attachment points between motors and electrical equipment. With all of this taken into account we can approximate a worst case hip length to be around 250 mm. This arrangement can be seen below in figure 11.

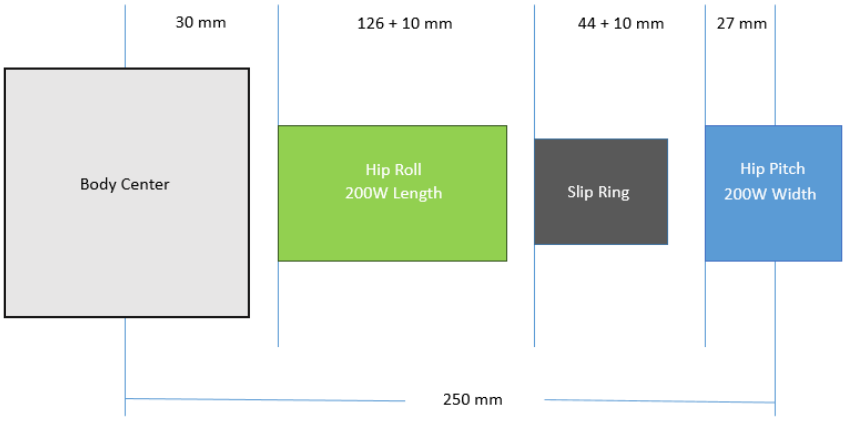

Figure 11 - Maximum Hip Span Estimate

Now that the stance geometry is defined we can look at other possible poses where the torque on specific actuators will be the highest. Fortunately, the worst case torque scenario for every joint type (hip roll, hip pitch, hip yaw, and knee pitch) is when the robot is mid-step. This is because while the system is mid-step it is only supported by two of the three legs which means the torques on the hip and knee pitch actuators will be higher than the torque in the equilibrium stance. Also during the step phase the hip yaw actuators will experience their highest torque when the body link is rotated so that it is perpendicular to the ground (figure 12). Finally, while the robot is mid-step the hip roll actuators in the stance legs will be rotating the body and swing leg through the two stance legs as fast as possible. The hip and knee pitch actuators of the swing leg will also be rotating during the step but will only be supporting the weight of the swing leg which will be negligible compared to the torque on the stance leg actuators in the same locations. With all of this in mind we can define a worst-case torque scenario as the point when the robot is mid step and the body link is perpendicular to the ground. This configuration is shown below in figure 12.

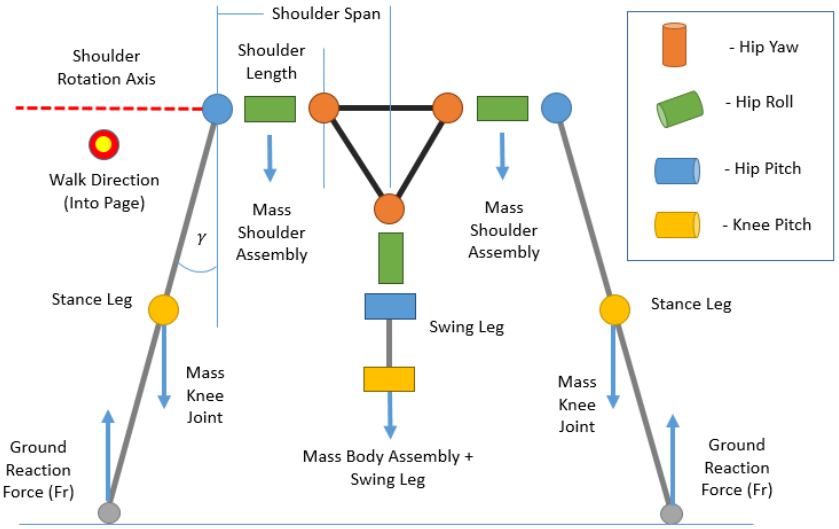

Figure 12 - Estimated Worst Case Torque Scenario Free Body Diagram

Now that the worst case scenario and body geometry is defined we can proceed to calculate the required joint torques to keep the fixed joints stable in the given pose. This can be done using simple statics calculations with approximated body masses and link geometry. The required joint torques can be found as follows by using the free body diagram shown in figure 12.

Firstly calculate the ground reaction force;

$$F_r \approx \frac{1}{2} g\left(M_{Body} + M_{Swing\ Leg} + 2M_{Shoulder} + 2M_{200W}\right) \tag{1}$$

Now calculate the joint torques;

$$\begin{aligned} Hip\ Yaw\ Torque \approx\ & F_r\left(L_{Shoulder\ Span} + H\sin(\gamma)\right) \\ & -g(M_{100W})\left(L_{Shoulder\ Span} + \frac{1}{2}H\sin(\gamma)\right) \\ & -g(M_{Shoulder})\left(L_{Shoulder\ Span}\right) \end{aligned} \tag{2}$$

$$\begin{aligned} Hip\ Pitch\ Torque \approx\ & F_r(H\sin(\gamma)) \\ & -g(M_{100W})\left(\frac{1}{2}H\sin(\gamma)\right) \end{aligned} \tag{3}$$

$$Knee\ Pitch\ Torque \approx F_r\left(\frac{1}{2}H\sin(\gamma)\right) \tag{4}$$

Where $H = Maximum\ Height\ of\ Robot$ and $\gamma = Hip\ Pitch\ Angle$

Given that this is the worst case scenario we will select the actuator for each joint with minimal torque required to withstand the scenario. The goal of which is to choose the smallest motors possible in order to minimize weight and power consumption for the whole system. The largest limitation comes from the slip ring selection since the largest slip ring that fit the requirements would only support at most a 100W actuator at the knee and a 100W actuator at the hip pitch joint. In addition we would like to keep the body section as light as possible so we will assume for now that a 20W actuator will suffice at the hip yaw

joint. Finally we assume that the torque on the hip roll joint will actually be quite low in practice since its primary use is to rotate the body and swing leg through the stance legs while taking a step. Thereforee we will assume this joint uses a 100W actuator as well. With this is mind we can calculate the approximate mass of the system and evaluate equations 1 through 4.

$$\begin{gathered} M_{Body} \approx\ 3M_{20W} + 3M_{Battery} + M_{Comp} + 0.2kg_{aluminum} \approx 2.0\ kg \\ M_{Swing\ Leg} \approx\ 3M_{100W} + 0.4kg_{aluminium} \approx\ 2.6\ kg \\ M_{Shoulder\ Assem} \approx\ 2M_{100W} + 0.2kg_{aluminum} \approx\ 1.7\ kg \end{gathered} \tag{4}$$

$$L_{Shoulder\ Span} \approx 0.3\ m$$

$$\therefore$$

$$\begin{gathered} Hip\ Yaw\ Torque \approx 29.5\ Nm \\ Hip\ Pitch\ Torque \approx 22.5\ Nm \\ Knee\ Pitch\ Torque \approx 12.2\ Nm \end{gathered} \tag{5}$$

Comparing these torques to the torques provided by the three sizes of actuators available reveals that the requirements cannot be satisfied with the chosen geometry and motor size selection.

Table 2 – Dynamixel PRO Torque Specifications

Motor Model	Torque (Nm)
20 W	5.6
100 W	21.1
200 W	39.2

The estimated joint torques were computed with very little factor of safety. Ideally we would like the joint torques to be well within the operating range of the motor. Unfortunately all of our assumptions in picking initial motor sizes for each joint were conservative in weight. We chose the smallest actuator (20W) for hip yaw and 100W motors everywhere else. From the torque calculations one can see that the 100W actuators would be barely sufficient to actuate the hip pitch joint and ideal in actuating the knee joint. However the 20W hip yaw actuator is grossly undersized to handle the expected 29.5 Nm load. Unfortunately the only way to remedy this with actuator sizing choice alone is to increase the estimated size of the hip yaw actuator to 100W and repeat the calculations. Doing so yields the following results;

$$\begin{gathered} M_{Body} \approx\ 3M_{100W} + 3M_{Battery} + M_{Comp} + 0.2kg_{aluminum} \approx 3.2\ kg \\ M_{Swing\ Leg} \approx\ 2.6\ kg \\ M_{Shoulder\ Assem} \approx\ 1.7\ kg \end{gathered} \tag{6}$$

$$\begin{gathered} Hip\ Yaw\ Torque \approx\ 34.1\ Nm \\ Hip\ Pitch\ Torque \approx\ 25.4\ Nm \\ Knee\ Pitch\ Torque \approx\ 13.7Nm \end{gathered} \tag{7}$$

Unfortunately, with the added weight of larger actuators for the hip yaw joint, the total system weight drastically increased and therefore the estimated required joint torques went up as well. In fact they have gone up so much that now the actuator selection for two of the three calculated joints is insufficient. To make matters worse the hip pitch actuator selection is insufficient and due to the limitations of the slip ring the motor size cannot be increased for that joint. In addition, the torque for the hip yaw joint has also increased significantly enough that the 100W motor selection for that joint is also insufficient therefore it would have to be increased to a 200W actuator. This in turn would increase the body weight even further. At this point the conclusion was drawn that problem of motor size selection cannot be solved with increasing or decreasing motor size alone. In fact given the current system geometry there is no combination of motor sizes that would yield a statically stable system. Furthermore, these calculations do not even take into account the centripetal forces of the body and swing leg rotating through the assembly which would add significantly more torque requirements for all the actuated joints. Thereforee we are left with the following options;

1. Add another gearbox to certain actuators to increase torque output.
2. Decrease the height of the system.
3. Remove the slip ring which would eliminate the power constraint on the knee and hip pitch actuators.
4. Return to the original motor selection configuration with 20W actuators for the hip yaw and 100W actuators everywhere else and add a mechanical lockout to the hip yaw joint while stepping to eliminate the peak torque on that joint.

These possible options where explored and the following conclusions where arrived upon.

1. Adding gearboxes may solve the torque problem but it may not. It would add torque to the joints however it would also add weight and mechanical complexity. Much design time would have to be expended to even determine if it was possible to increase the torque enough to compensate for the added weight. This option should be explored if no other option is more feasible.
2. The effect of decreasing the height of the system is easily observed by recalculate the above two scenarios with a different system height. We shall see what happens if we make a substantial change to the system height by changing from a 3 meter height to 1.5 meters.

Table 3 – Comparison of System Height with Joint Torques

Joint Torque (Nm)	1.5 m System Height w/ 20W Hip Yaw Actuator	1.5 m System Height w/ 100W Hip Yaw Actuator
Hip Yaw	18.3	21.4
Hip Pitch	11.3	12.7
Knee Pitch	6.1	6.8

These results show that the configuration with 1.5 meter total height and 100W actuators in the hip yaw would be barely feasible but still not within a reasonable operating range. The 20W configuration is still outside the operating range of the 20W actuator. Thereforee neither configuration is ideal.

3. Removing the slip ring would eliminate the possibility for more than two or three consecutive steps which would limit the scope of the project too far short of its original goal.

4. Adding a mechanical lockout to the system would eliminate all torque on the hip yaw actuators while stepping which would allow use of the 20W actuator in any height configuration. This comes at the expense of overall mechanical complexity.

The only feasible options are 1 and 4. Each potentially solves the torque problems but comes with a downside of added weight and mechanical complexity. With this said however one option seems to be a much simpler implementation. Designing a reliable gearbox can be very time consuming and requires many individual components (shafts, gears, bearings, etc). Also in order to withstand the torques required there is a good chance all components would have to be made of steel and of a large size. This means lots of added weight. The mechanical lockout can potentially be done with far fewer moving components and could all be made out of aluminum. In addition the mechanical lockout would allow very precise alignment of the hip roll actuators. Finally the mechanical lockout would take all the load off of the hip yaw actuators mid step and thereforee the hip yaw actuators could actually be torqued off for the entirety of the step and while standing in certain configurations; therefore saving large amounts of power. Given the above information it was decided to use a 20W actuator for the hip yaw joint and implement a mechanical lockout during the step phase at a later date. All other joint actuators would be 100W actuators.

2.3 HIP DESIGN

The first sub-assembly to design is the hip. The reason the hip assembly is tackled first is because it houses 9 of the 12 actuators, slip rings, a number of bearings, and interfaces with both of the other sub-assemblies (Body and Leg). This makes it the most complicated assembly in the system. Thereforee this assembly can be designed first and the rest of the robot can be designed, more or less, around it.

The first step in the design process is to orient all of the necessary components in a realistic manner in CAD and visualize how best to fix them to one another. There is also a wealth of information to be drawn from previous iterations of the same platform [1-7]. The most important of these considerations is the relationship between hip span and the clearance between the swing foot and ground during the step. The longer the hip assembly the more the robot has to bend the knee of the swing leg in order for the foot to clear the ground. Therefore, there is an inverse relationship between hip span and ground clearance. This can be seen in figure 13 and 14.

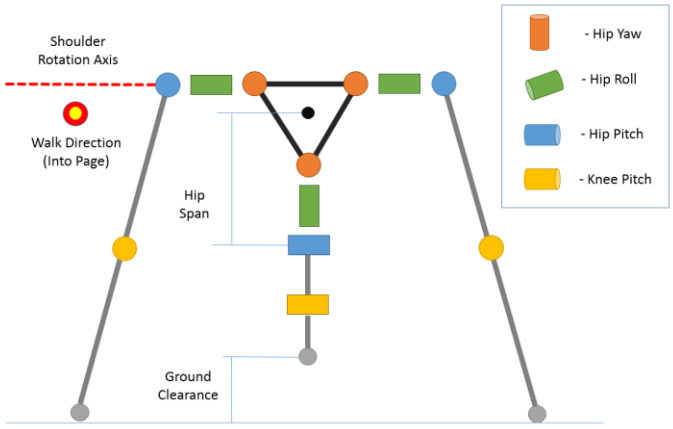

Figure 13 - Front view mid-step

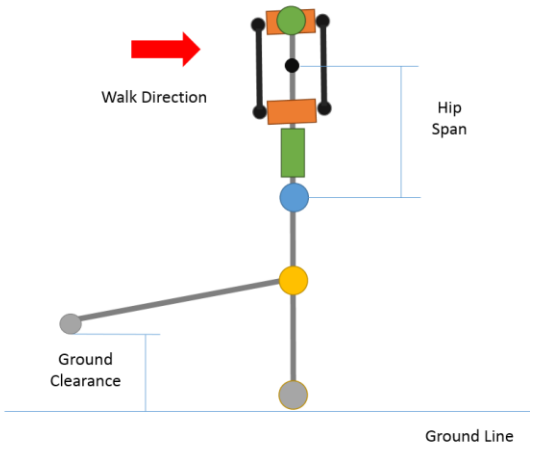

Figure 14 - Side view mid-step

With this relationship in mind, we can draw out the approximate arrangement of the hip joint and its components as follows;

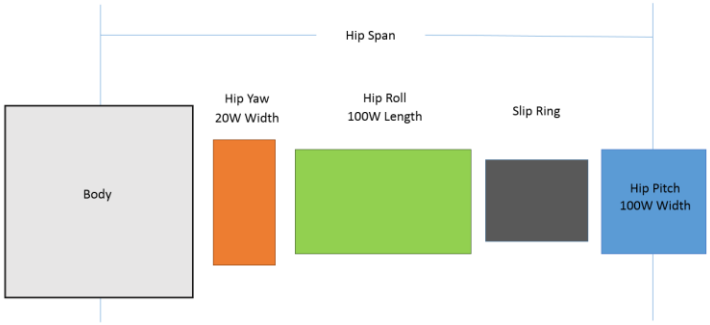

Figure 15 – Hip span in arrangement 1

Due to the through-bore of the slip ring it can be most easily and sturdily mounted in line with the hip roll axis and should therefore probably not be moved from its currently assumed position. The shaft would be running through the slip ring and needs to be mounted to the hip pitch motor in some way. Ideally the gap between these two parts should be as small as possible. Again the easiest way to accomplish this is to have the hip pitch motor directly in-line with slip ring shaft. One interesting change to explore in the component orientations in figure 15 is to move the hip yaw actuator. We have great freedom in doing this because there is no particular reason the actuator should be in line with anything in the plane of figure 15. If the overall goal is to shorten the length of the hip span then, ideally, we should remove the hip yaw actuator from being in-line with the other components of the hip and move it either above or below the rest of the assembly. This arrangement can be seen below in figure 16.

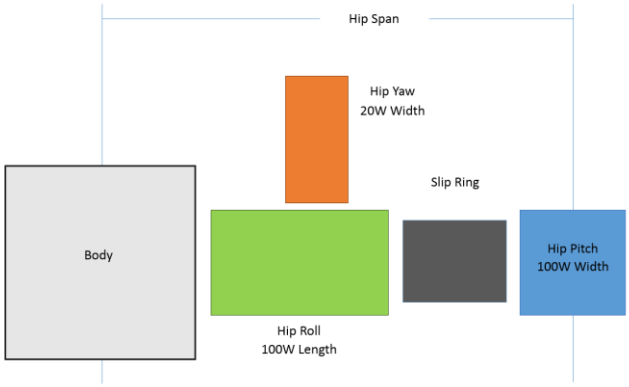

Figure 16 – Hip span in arrangement 2

One can see that the hip span has now been decreased by approximately the width of the hip yaw actuator. Now, however, this raises the question of where exactly should the hip yaw actuator be located in this orientation. The positioning can range anywhere from the left side of the hip yaw actuator being in-line with the left side of the hip roll actuator to the right side of the hip yaw actuator being in-line with the right side of the hip pitch actuator. There are three important factors to consider when evaluating this decision. The first of which is that since the hip yaw actuator is necessarily the first actuator in the chain of joints, the farther away from the body the hip yaw joint is located the farther away the mounting location of that actuator is from the center of the body. This means the body itself will have to be larger (increased weight and material) and the bending moment between the body and hip yaw actuator will be larger because the moment arm between adjacent yaw joints is larger. This is illustrated below in figure

17 where the narrow configuration represents the configuration with the hip yaw actuator as far towards the inside of the hip assembly as possible and the wide configuration with the yaw actuator as far towards the outside of the hip assembly as possible. Clearly the "body width" increases and so to does the bending moment between adjacent yaw joints.

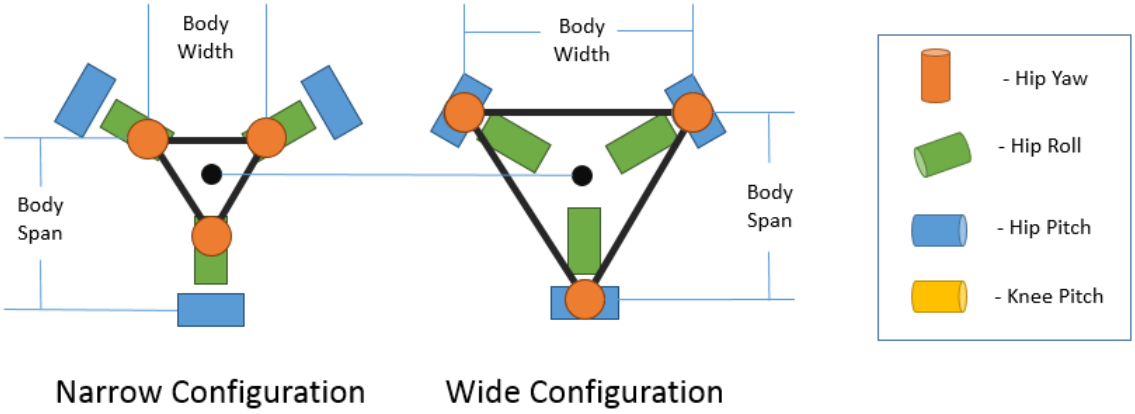

Figure 17 – Comparison of Hip Configurations With Body Width

One can also draw another conclusion between the narrow and wide configuration which is the difference in "body span". This dimension is important in that it also affects ground clearance during a step. The larger this dimension the more the swing leg has to bend in order to clear the ground. These two factors so far reflect that the narrow configuration is preferable to the wide configuration, however there is one more factor to consider and that is the distance from the hip yaw actuator to the hip pitch actuator. This dimension is detailed below in figure 18 as "dimension 3".

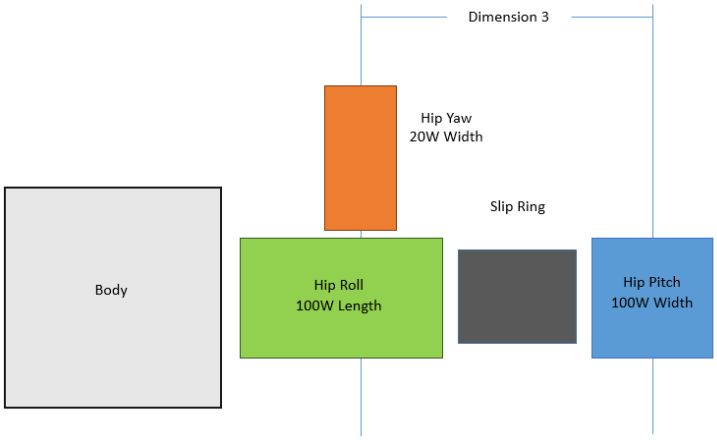

Figure 18 – Dimension 3 effect on hip geometry

The larger this "dimension 3" is the larger the torque required for the hip yaw actuator operate. In the previous section it was decided to use the smallest of the three actuators (20W) at this joint due to weight and power limitations. Increasing the size of dimension 3 would only exacerbate the already high loads on the small actuator. Therefore we would like to keep this distance as small as possible. If we increase dimension 3 then the bending moment on the body structure will be less and the ground clearance will be maximized however if dimension 3 is decreased then the torque required at the hip yaw joint will be lower. In addition due to the nature of the problem there is most likely no "optimal" solution because the

result of the optimization would be purely based on how the designer weighs the importance of these characteristics with respect to one another which is subjective. The most important consideration may be how well this configuration fits in with the rest of the body assembly. There seems to be no clear wrong or right answer as to where exactly the hip yaw actuator should be located and the best location is probably somewhere in between the narrow and wide configuration of figure 17. Thereforee it was decided to build an adaptable assembly in CAD where the location of the hip yaw actuator could be easily changed and the body assembly, once designed, could change around it accordingly. This would allow for quick experimentation of the placement of other components in the body itself to try to find a "global solution". This solution would also be able to take into account other less objective factors such as ease of assembly, manufacturing, and wiring. In addition there are factors of the body design which can also greatly influence the hip design. Namely the need to balance the body assembly about the mid-plane axis of the body for repeatable gaits (this will be detailed in the following section). Therefore the overall design of the hip assembly should took place in parallel with the body design.

From this point the actual CAD design can begin and one can start looking at the details of how to put this assembly together. The process of which is outside the scope of this report. There is no perfect mechanical design and possibly infinite solutions. The overall goal of this process is to minimize weight, hip span, components, fabrication time, and assembly time, while maximizing strength and rigidity. In addition it was also important to keep in mind how the hip assembly may eventually connect to the body and leg assemblies. The final design can be seen below in figure 19 and 20.

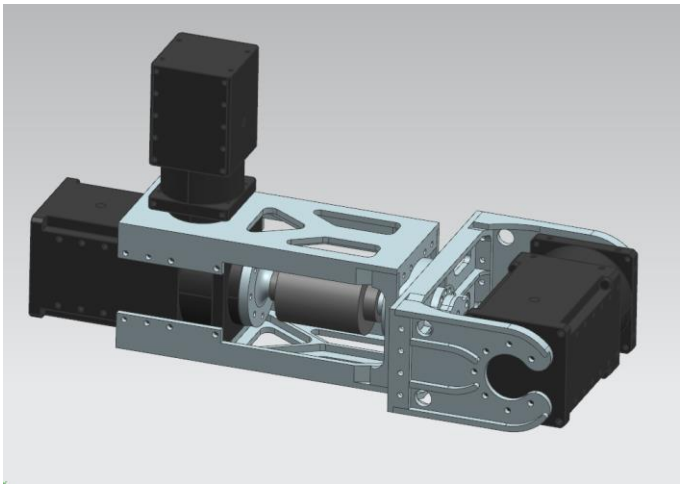

Figure 19 – Completed CAD Drawing of Hip Assembly

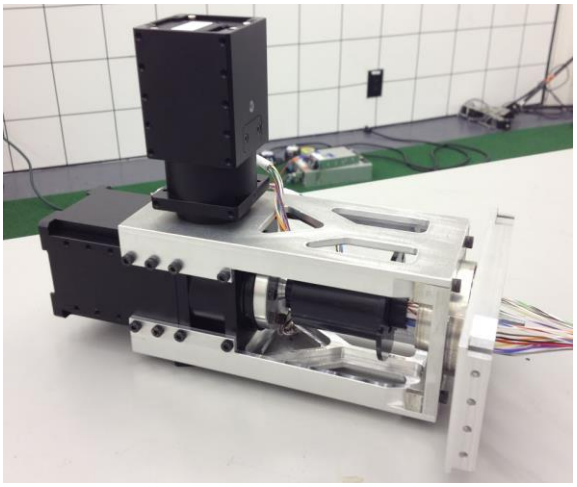

Figure 20 – Assembled Hip Assembly

The most difficult consideration in the final detailed design of the hip is the inclusion of the slip ring and how to transfer the wires from the output of the slip ring to the input of the next joint, namely the hip pitch actuator. Numerous different methods were explored but the final solution was to remove the inner race from a needle roller bearing and machine another, slightly thicker, with a smaller inner diameter, so that the inner race of the bearing itself could be drilled with lengthwise holes to accommodate all 24 wires leaving the slip ring. These wires would then be allowed to pass through the mechanical joint itself without getting tangled up in any rotating parts. The final design of the drilled out bearing can be seen below in figure 21 and 22.

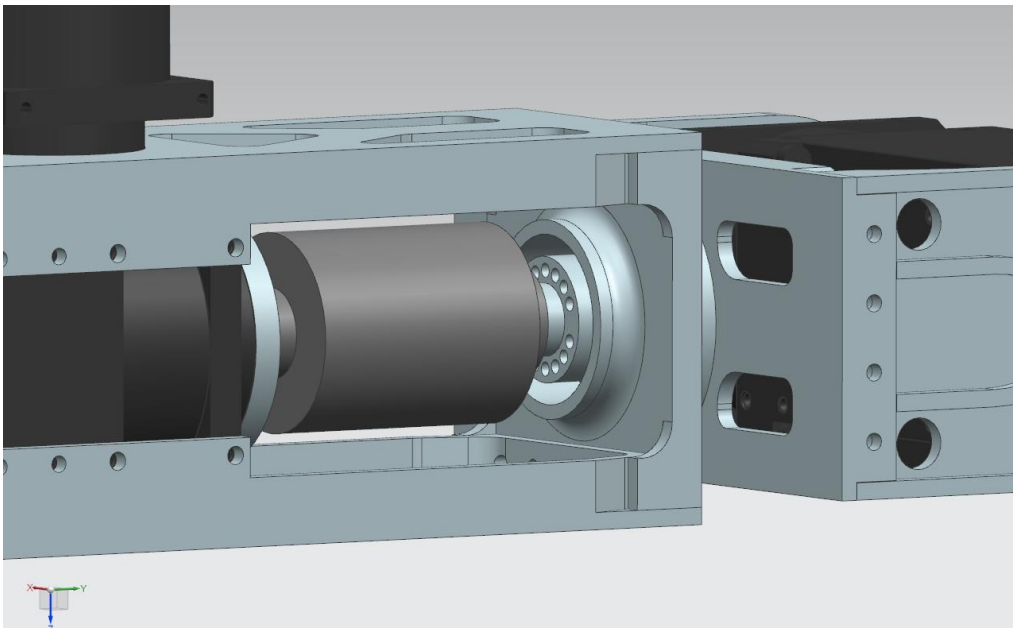

Figure 21 – Slip Ring Design Detail

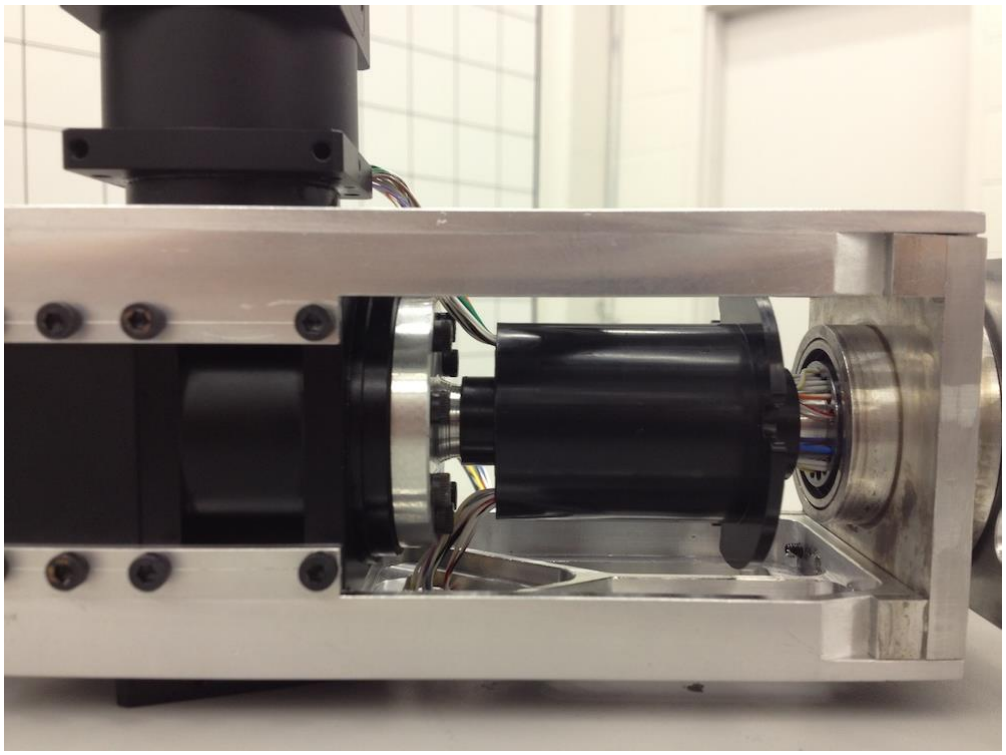

Figure 22 – Assembled and Wired Slip Ring Assembly

The next design consideration of the hip joint was the inclusion of a thrust bearing in the interface between the hip-roll/slip-ring assembly and the hip pitch joint. This was included to help the assembly withstand the high bending moments and forces from the stance legs which connect directly through the hip pitch actuator. Using equation 3 the bending moment at the location in question was estimated to be approximately 22.5 Nm and the thrust bearing was sized accordingly with a reasonable factor of safety. The final design of the thrust bearing assembly can be seen below in figure 23. The inner race of the

thrust bearing had to be oversized in order to accommodate the wires leaving the slip ring and radial bearing assembly.

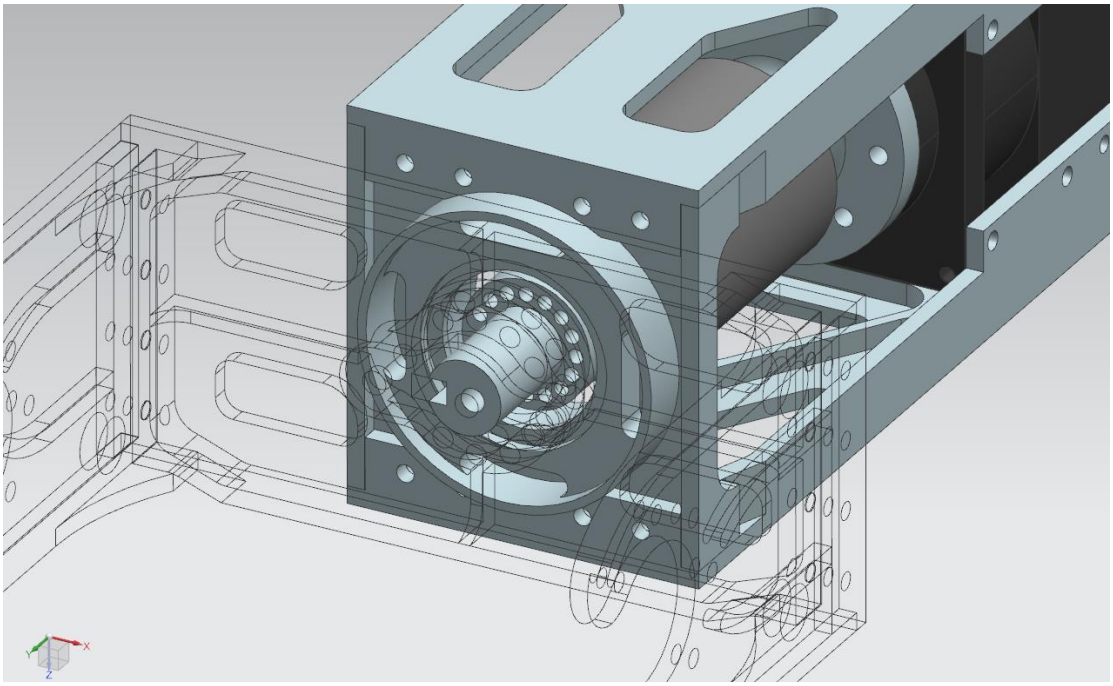

Figure 23 – Thrust Bearing Detail View

The final design consideration was the sizing and attachment method of the shaft leaving the hip roll actuator and going to the hip pitch actuator. The through bore of the slip ring was exactly ½ inch therefore for ease of assembly and manufacturing a $\frac{1}{2}\ inch$ aluminum shaft was assumed. The attachment method was decided to be a $\frac{1}{8}\ inch$ keyway with oversized key to hopefully eliminate the possibility of backlash even after significant use and keyway deformation over time. A basic hand calculation of the shaft and keyway was performed in order to validate the choices of shaft and keyway size. These can be seen in appendix A and B respectively.

In addition both a radial bearing and a thrust bearing were included at the hip roll joint to withstand the large bending moment on the structure. An exploded view of the entire hip assembly can be seen in figure 24. The slip ring is shown in green. The radial bearing is shown in yellow. The thrust bearing is shown in red.

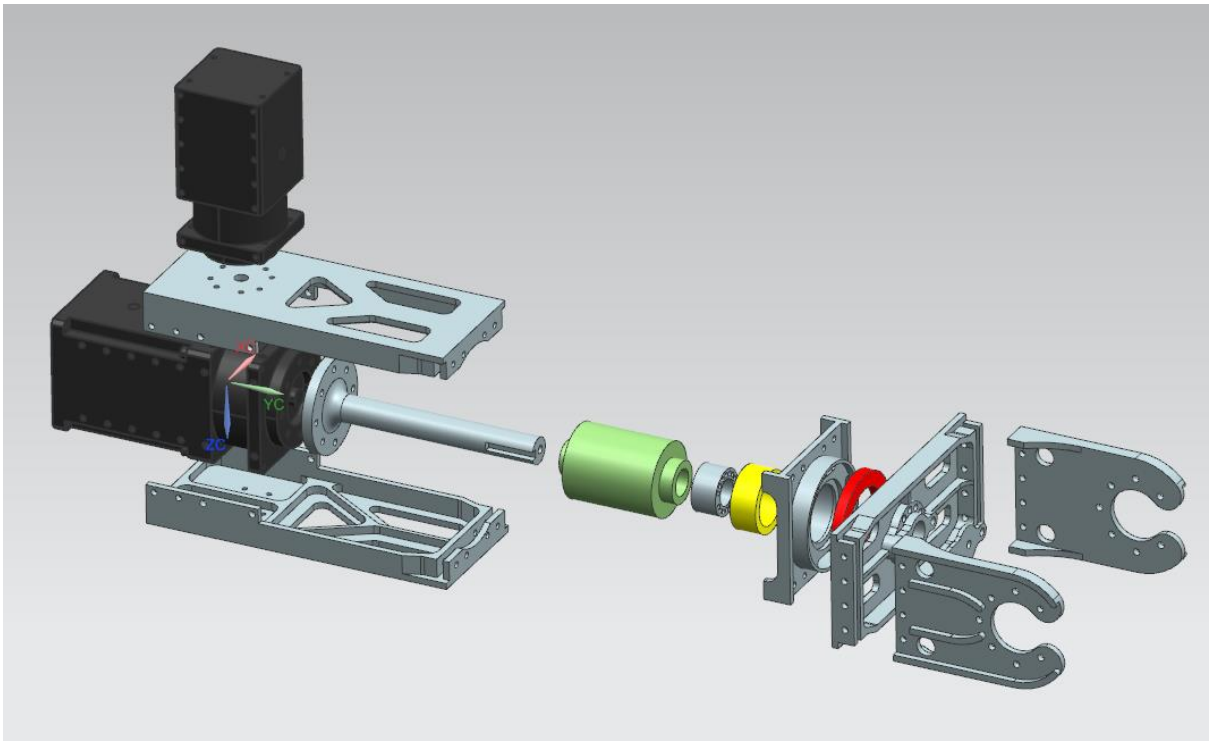

Figure 24 – Exploded View of Hip Assembly

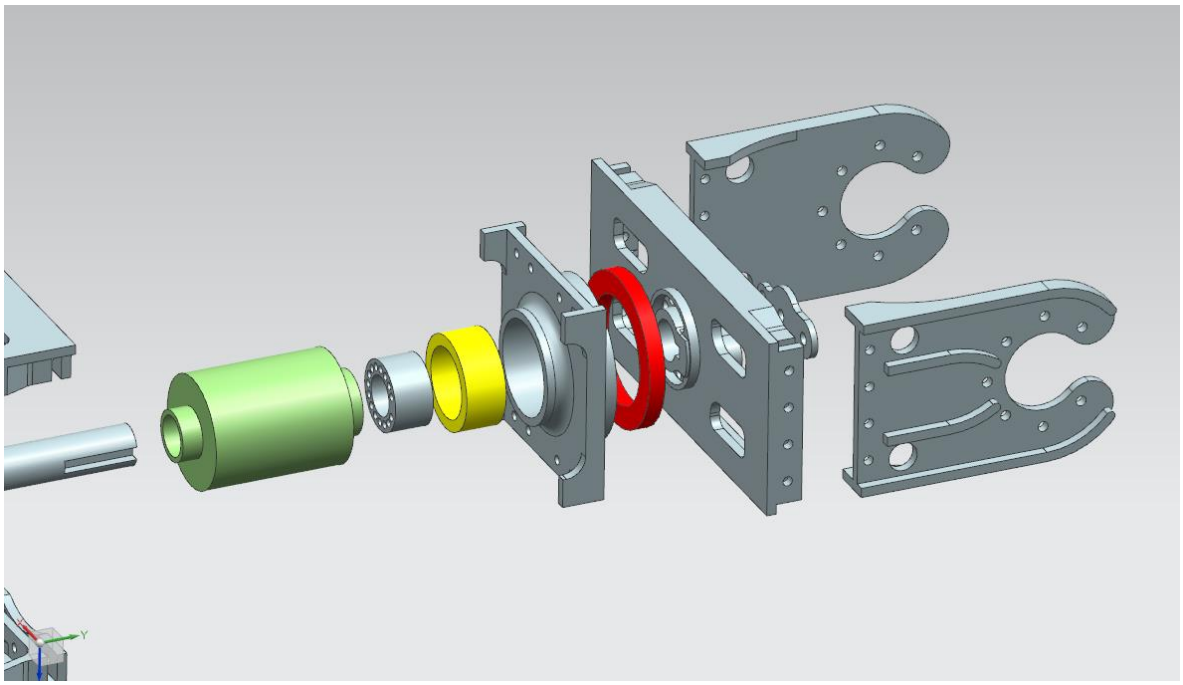

Figure 25 – Exploded View of Hip Bearing Assembly

2.4 BODY DESIGN

Unlike the hip design, there were very few equations involved with the design of the body. It was mostly a packaging problem where enough space is needed for all the parts and components to fit and move around without contacting one another. There had to be space for wires to be routed without catching on moving parts. In addition, the assembly had to be easy to manufacture, assemble, and service. These are all factors that involve little to no equation solving and is mostly an exercise in trial and error, patience, and experience. With this said however, there were two critical concerns in the design of the upper body that did require extra consideration. These two factors being the requirements of symmetrical weight distribution about 4 different geometric planes and the need for the complete assembly to be sufficiently rigid and strong. The consideration of these two factors will be discussed in further detail below.

2.4.1 BODY SYMMETRY

In previous sections the novel gait strategy of the THALeR platform has been discussed and it was highlighted how one of the more unique aspects of the gait is once the feet are on the ground the robot is only capable of stepping in one of three directions shown in figure 26. Once a walk direction is chosen the hip axis of the stance legs are aligned as seen in figure 27.

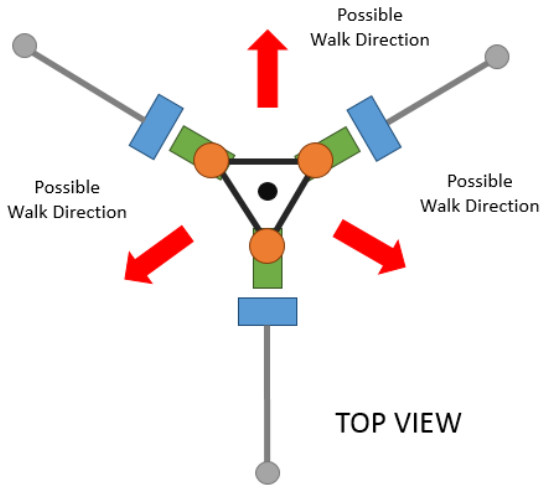

Figure 26 – Top View of THALeR in Equilateral Stance and Possible Walking Directions

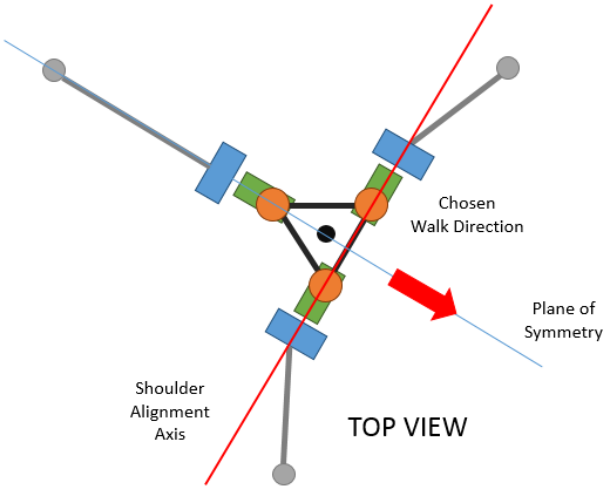

Figure 27 – Top View of THALeR in Hip Aligned Stance and Chosen Walk Direction

In order for the step to complete successfully the weight must be balanced along the vertical plane containing the swing leg (Plane of Symmetry). Therefore the body assembly needs to be symmetrically weighted about all three possible planes containing all three swing legs. This geometry is shown in figure 28.

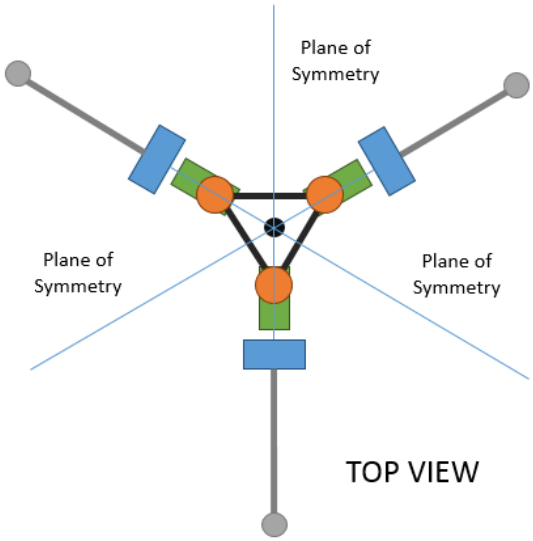

Figure 28 – Required Planes of Symmetry in Top View of THALeR Platform

These three planes are not all the planes about which the body must be symmetric. The robot also needs to be able to take continuous steps. For every consecutive step the body link flips 180 degrees. Thereforee if the body link is not balanced about the plane containing the hip roll axis, the dynamics of the system will be different during every other step. This can be compensated for by the controller but it would imply that two separate controllers depending on how the body link is oriented during the step. If however the body link is symmetric about the hip roll plane, then one can use a controller independent of step direction. The hip roll plane can be seen in figure 29.

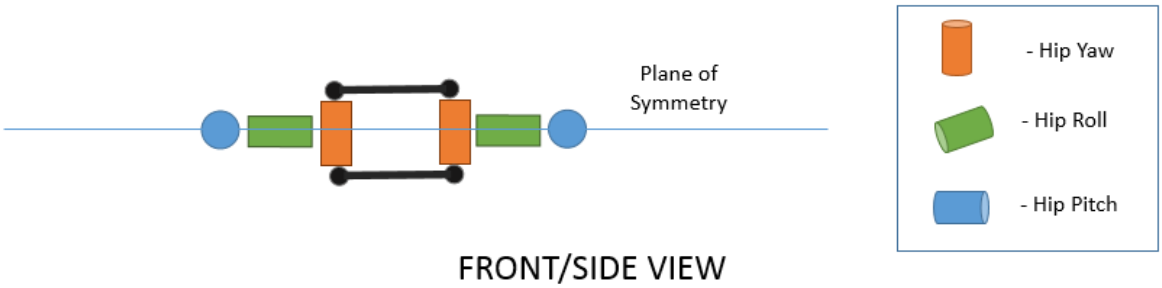

Figure 29 – Required Plane of Symmetry in Side View of THALeR Platform

With the planes of symmetry known we can proceed to arrange the different components to obtain approximate mass symmetry between the four planes described. The options for arranging these components in such a fashion were very limited therefore only the decision process for the final designed used will be described in detail.

Firstly, we look at the front/side view of the body assembly with the previously designed hip arrangement included. The primary function of the body assembly is to securely attach all three identical hip assemblies to one another while provided mounting locations for the batteries, computers, and sensors. An approximate configuration of the hips in an otherwise empty body assembly is shown in figure 30.

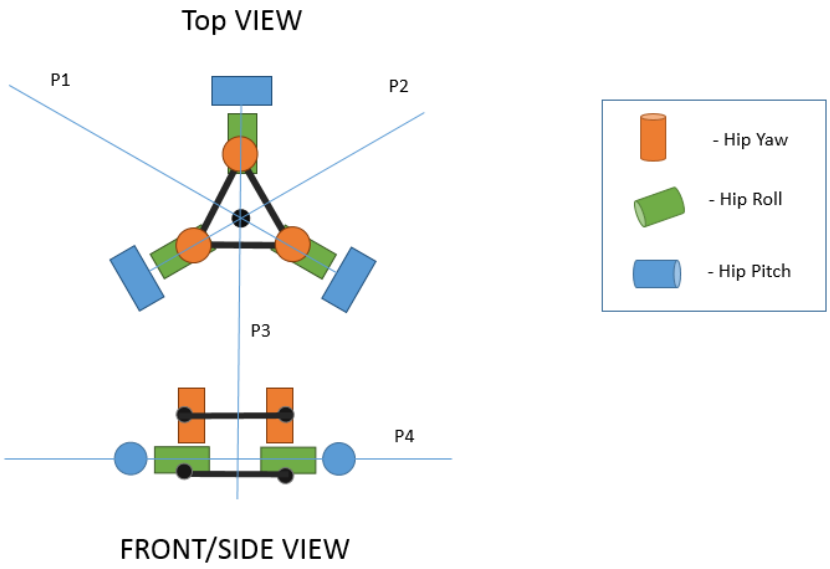

Figure 30 – Body and Shoulder Assembly With Required Planes of Symmetry and no Batteries or Computers Mounted.

The most important thing to notice in Figure 36 is how the hip yaw actuators stick out above the hip roll joints in the front/side view. This means that we have an issue with the assembly not being balanced about plane 4 (P4). We are however symmetric about planes P1, P2, P3. Therefore whatever components we add should maintain symmetry about these planes while still attempting to add mass below plane P4 to balance the mass of the hip yaw actuators above plane P4.

The hip haw actuators are quite heavy compared to the components that have to be located on the body. Therefore only components of significant enough mass will effect the off-plane weight distribution caused by the placement of the hip yaw actuators. The only components of significant mass to consider are the batteries and the computer, hence we need to place these components in order to balance the mass of the hip yaw actuators. The design of the hip assembly is far enough along to know the exact location of the center of mass of the hip yaw actuators above plane P4. Ideally, the batteries should all be located at the same height relative to plane P4. Therefore we can vary the height of the batteries ($z_{batteries}$) and computer ($z_{computer}$) relative to P4 until the system is balanced. A diagram of this is shown in figure 31.

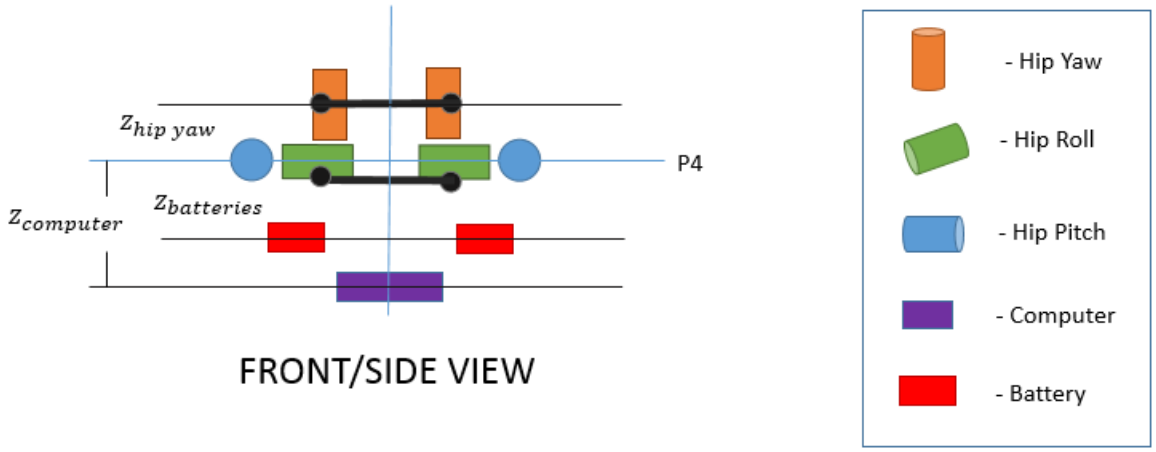

Figure 31 – Side View of Platform Showing Height Offsets for Necessary Components to Balance Mass About Horizontal Plane of Symmetry P4.

An equation describing the average center of mass of the system is as follows;

$$m_{hip\ yaw} z_{hip\ yaw} = m_{batteries} z_{batteries} + m_{computer} z_{computer} \quad (8)$$

This is a single equation with two unknowns therefore infinite solutions. However it is know that we would like to limit all heights z while leaving enough room for the hip assemblies to rotate freely. Since none of the components can fit in the space between both hip roll actuators both components must be located below the hip roll actuator. Since the mass of the combined batteries is much greater than the mass of the computer we will place the batteries as close as possible to the hip roll actuators which fixes the value of $z_{batteries}$. This then allow us to solve for $z_{computer}$ to render the system balanced about plane P4.

Next we need to place the computers and battery in the top view. This means we have to balance all three batteries and single computer about 3 planes at 120 degree angles with one another. Conveniently there are three batteries and three planes (this was actually intentional). This means there are only two possible solutions to this problem however one is ruled out by our choice of mounting heights just described. The two possible solutions are shown below in figure 32.

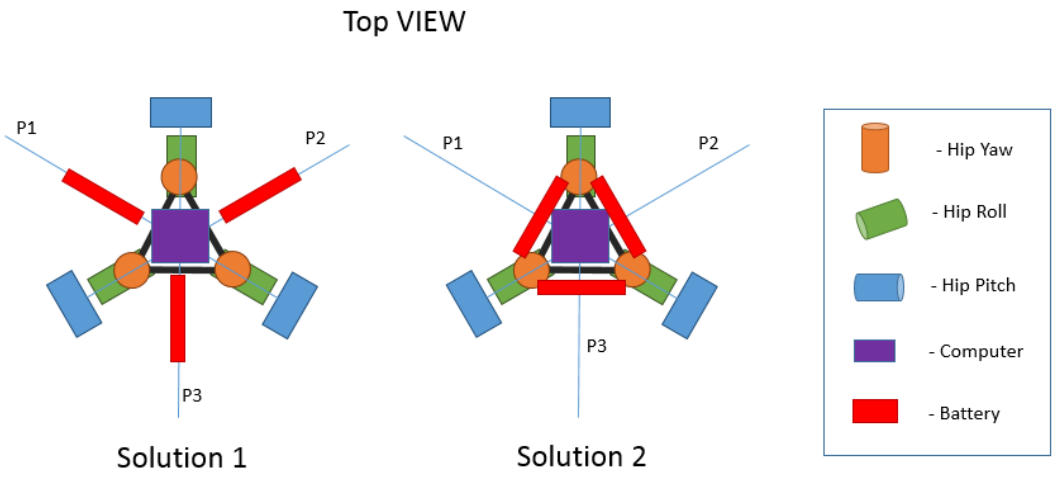

Figure 32 – Possible Mass Symmetric Mounting Positions for Batteries and Computers

Clearly the preferred solution from a packaging perspective is solution 2. The will allow a much smaller body assembly and also make it easy to protect the batteries from impacts. With the approximate locations of the components known, the detailed design of the body and hip assembly could continue. Again the method about which detailed design was completed is outside the scope of this text. The overall goals were to minimize weight and size while maximizing strength and rigidity. In addition, the exact radial location of the hip yaw actuator was determined during this process as well as other concerns such as wiring, assembly and manufacturing. For manufacturing almost all aluminum parts were designed to be "single sided". Meaning all milling operations could be performed with the cutting tool in a single orientation with respect to the work piece; this minimizes fabrication time. The final design of the body and hip assemblies can be seen in figures 33 to 38.

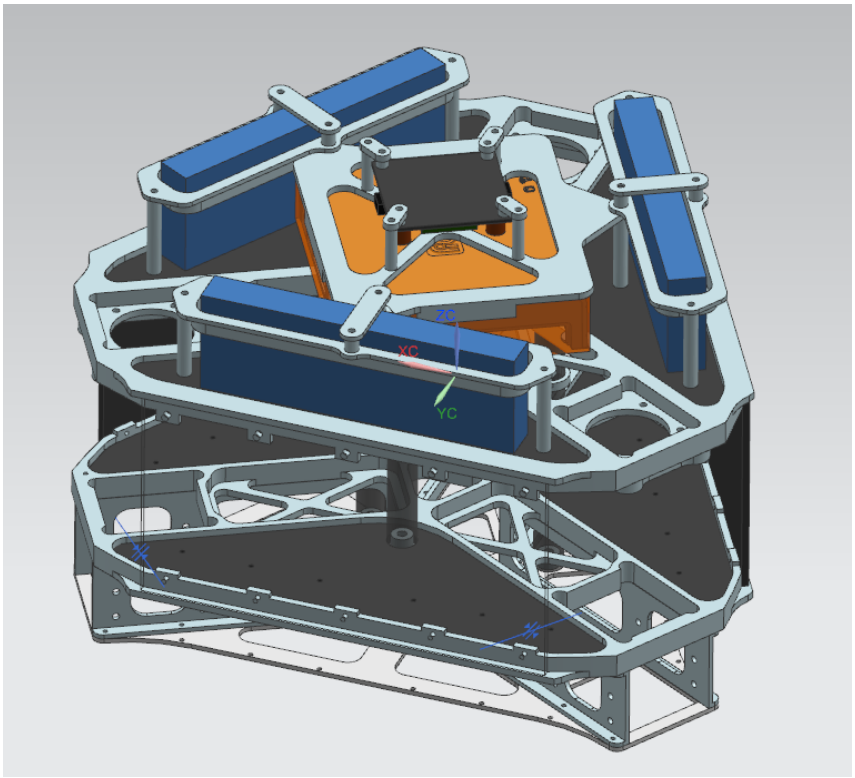

Figure 33 – CAD View of Bottom Side of Body Assembly

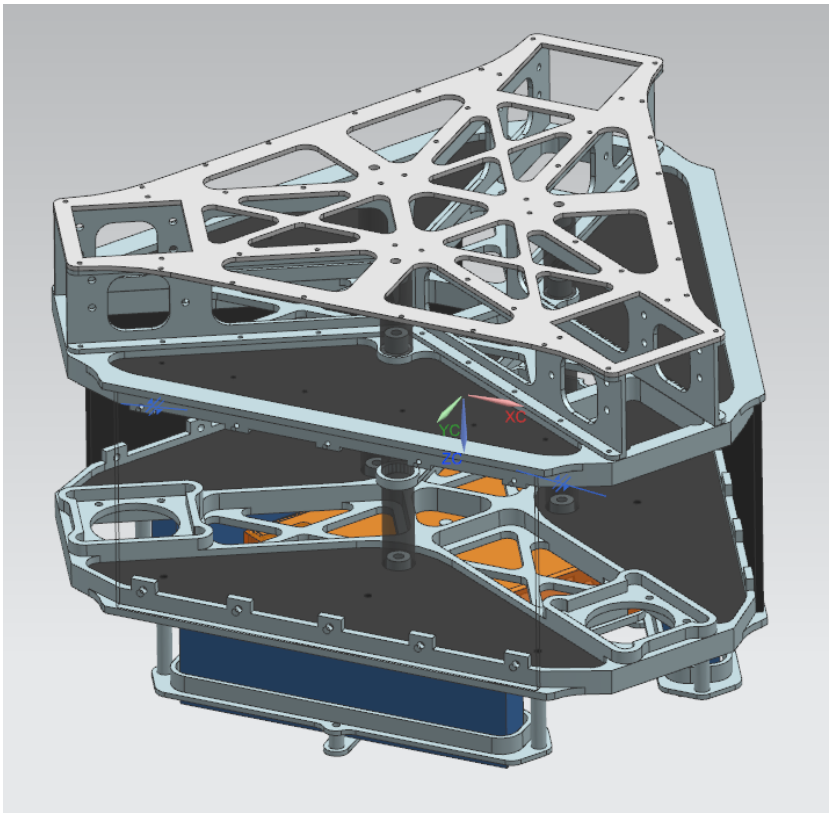

Figure 34 – CAD View of Top Side of Body Assembly

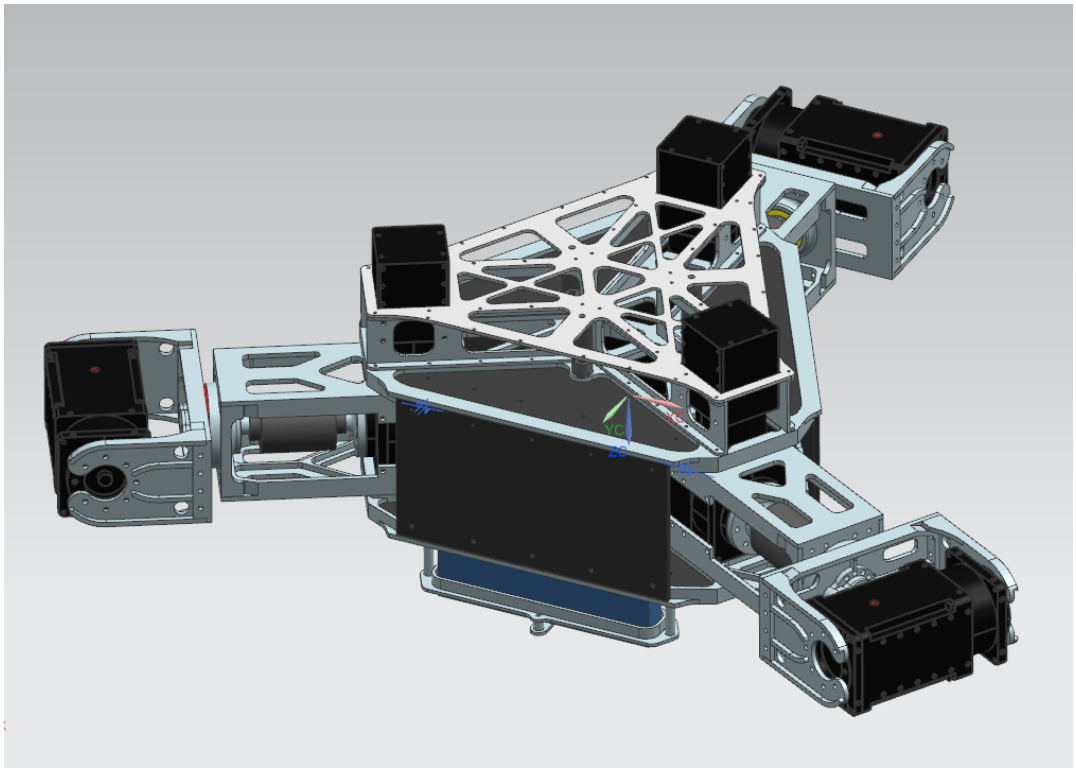

Figure 35 - CAD View of Bottom Side of Body and Hip Assembly

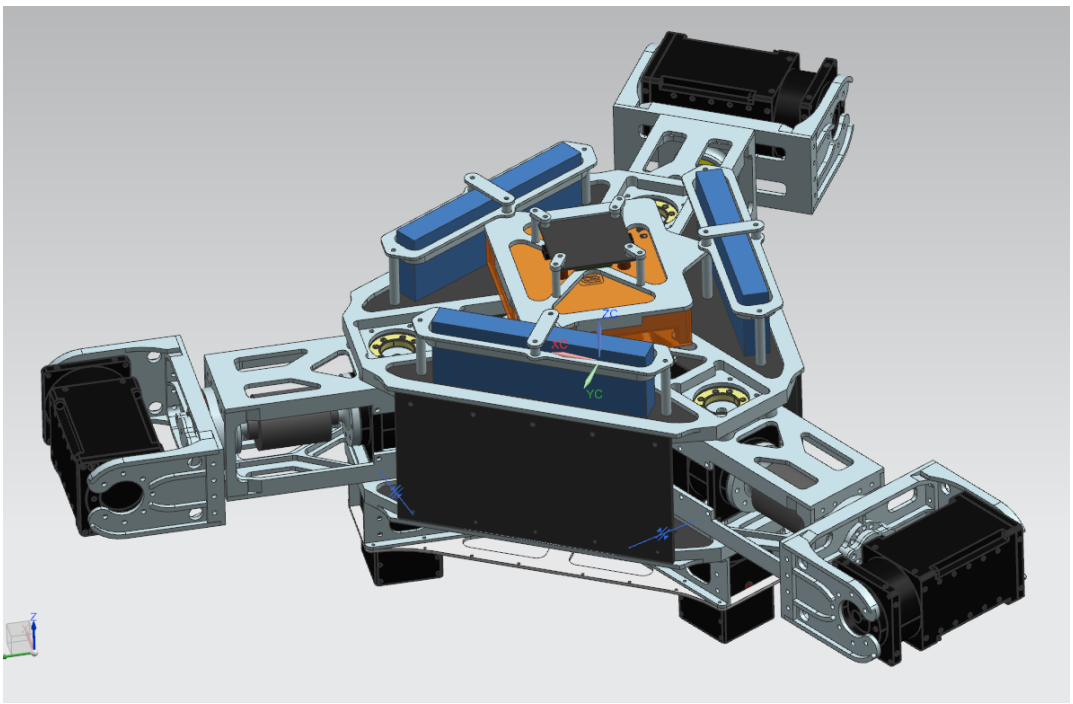

Figure 36 - CAD View of Top Side of Body and Hip Assembly

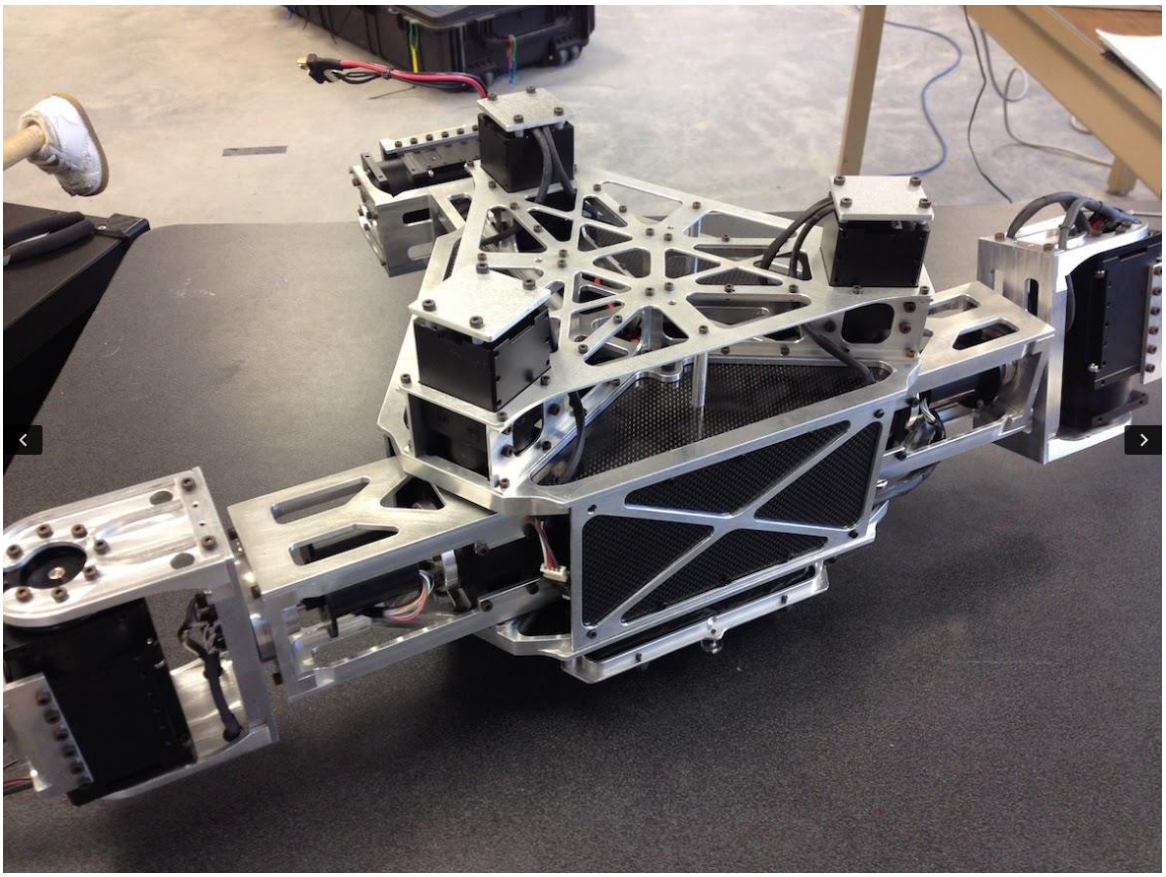

Figure 37 – Completed View of Bottom Side of Body and Hip Assembly

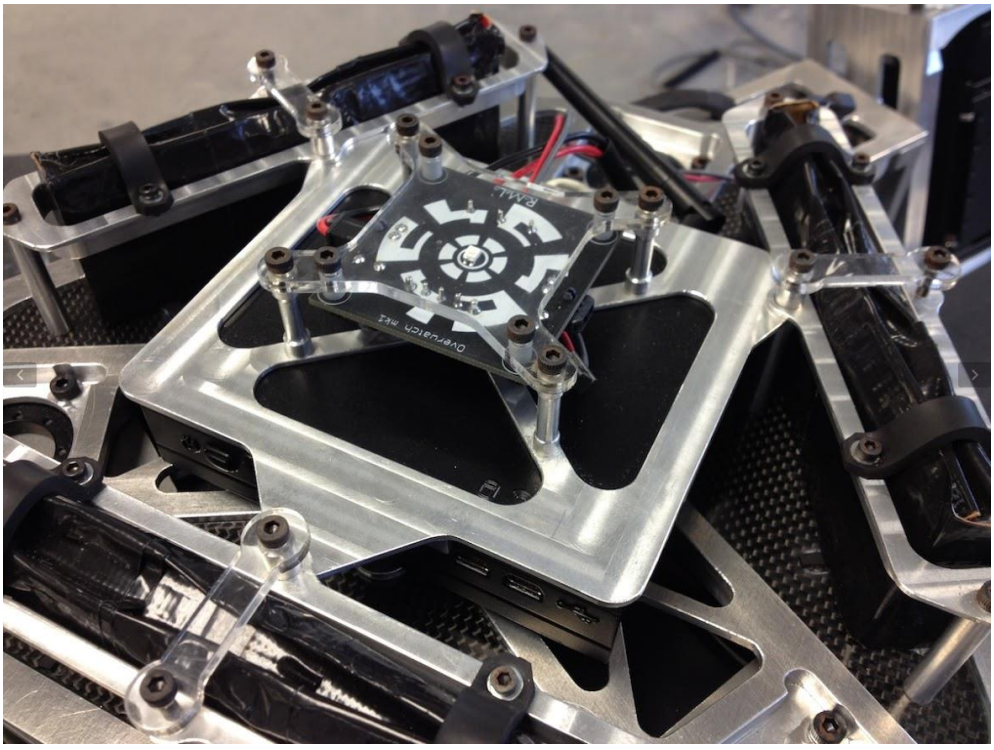

Figure 38 - Completed View of Bottom Side of Body and Hip Assembly

2.4.2 BODY FINITE ELEMENT ANALYSIS

The structure of the body assembly and shoulder joints is very complicated and difficult to analyze for strength and rigidity by hand. The quickest and easiest method to do this is by using Finite Element Analysis (FEA) to get a general sense if there are any grossly over-designed or under-designed sections. The main considerations in FEA analysis is how to load and constrain the model. In order to simplify analysis the shoulders and body assembly will be considered as one solid body. All connection points will be filled and united. The complete body will be loaded in two configurations.

2.4.2.1 CONFIGURATION 1

The first configuration simulates the system while standing in the equilateral stance in figure 2. The system will be constrained via cylindrical constraints at the hip pitch joints. A bending moment also about the hip pitch joints will also be applied, which will be three times the value applied while standing (60 Nm). In addition the force of gravity will be magnified by three. The free body diagram of the system can be seen in figure 39. The NASTRAN constraint model can be seen in figure 40 and the NASTRAN load model can be seen in figure 41. The final results of the analysis can be seen in figure 43 and 44.

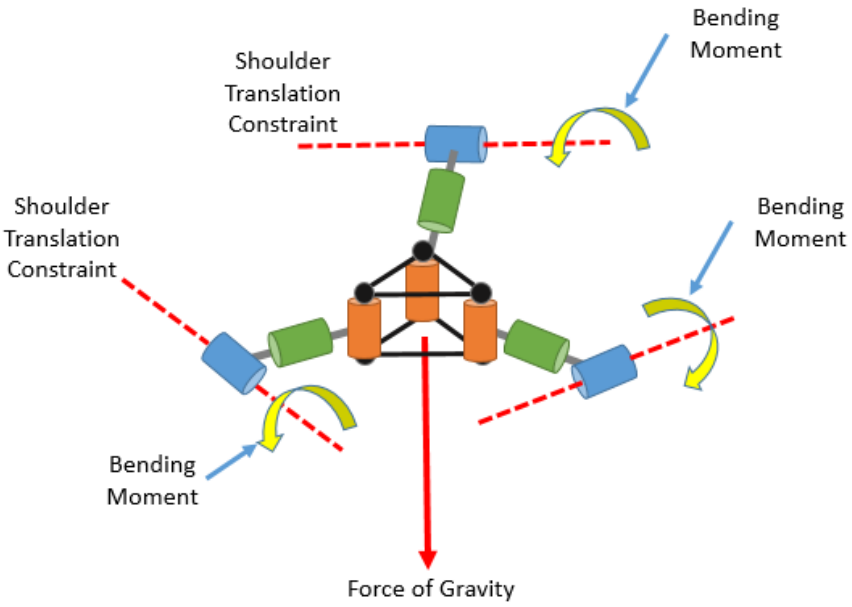

Figure 39 – FEA Configuration 1

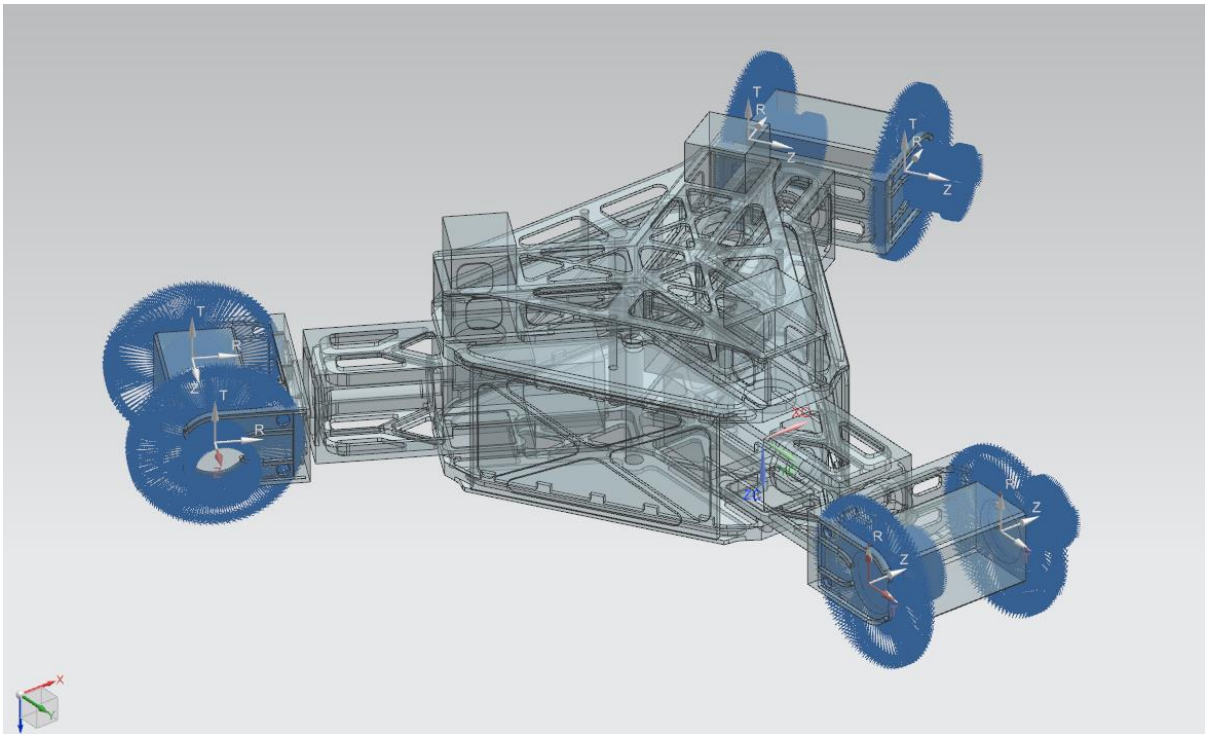

Figure 40 – Constraints Rendered in FEA Model of Configuration 1

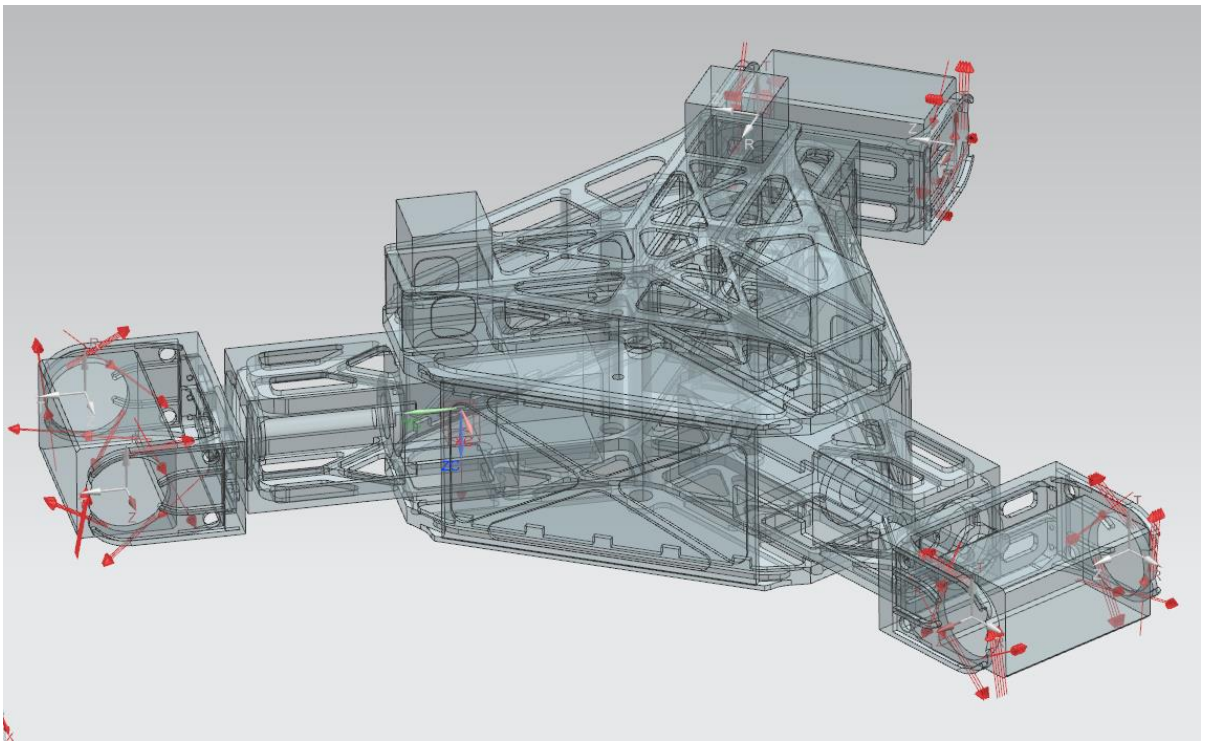

Figure 41 - Loads Rendered in FEA Model of Configuration 1

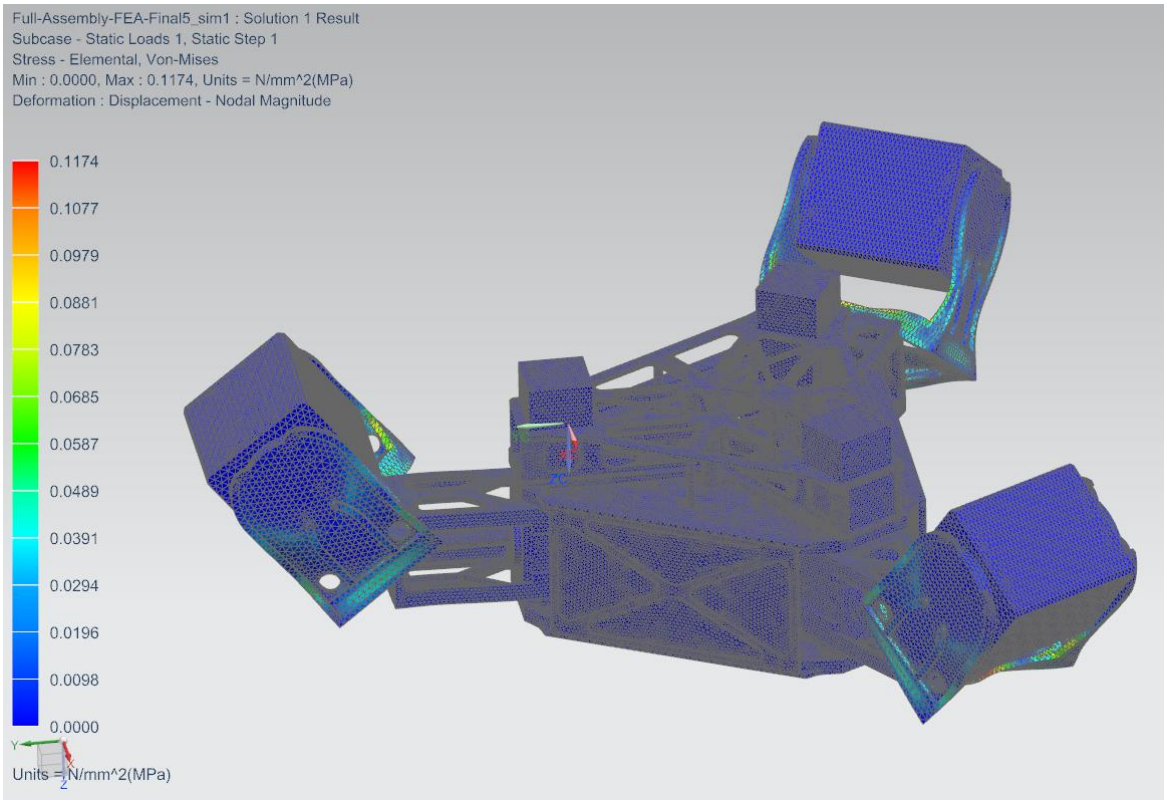

Figure 42 – Resultant Stresses in Configuration 1

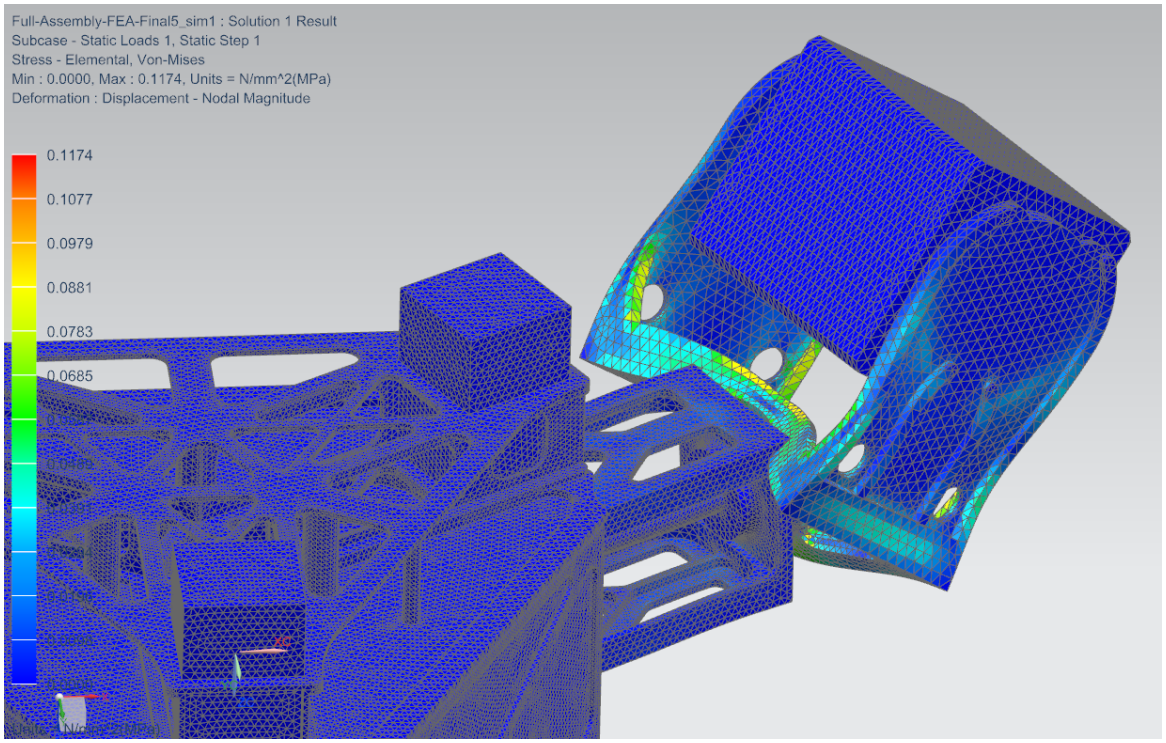

Figure 43 – Detailed View of Resultant Stresses in Configuration 1

2.4.2.2 CONFIGURATION 2

Configuration 2 simulates the system while in the mid-step state of figure 12. We will approximate the dynamic system by approximating the centripetal loads generated during the gait and applying them as static forces along with all gravitational forces and loading moments. We will constrain the system similarly to case 1 except the system is in a different configuration with the stance legs hip roll axis aligned and only the stance leg hip pitch axis will be constrained. The swing leg will be loaded with the weight of the rest of the swing leg plus centripetal forces of the swing leg with a factor of safety (200 N). Additionally, in both, cases bending moments proportional to the reaction moments of the stance legs will be applied to the shoulder pitch joints of the stance legs (100 Nm). Finally the force of gravity will be applied and multiplied by 3. The NASTRAN constraint model can be seen in figure 44 and the NASTRAN load model can be seen in figure 45. The final results of the analysis can be seen in figure 46 and 47.

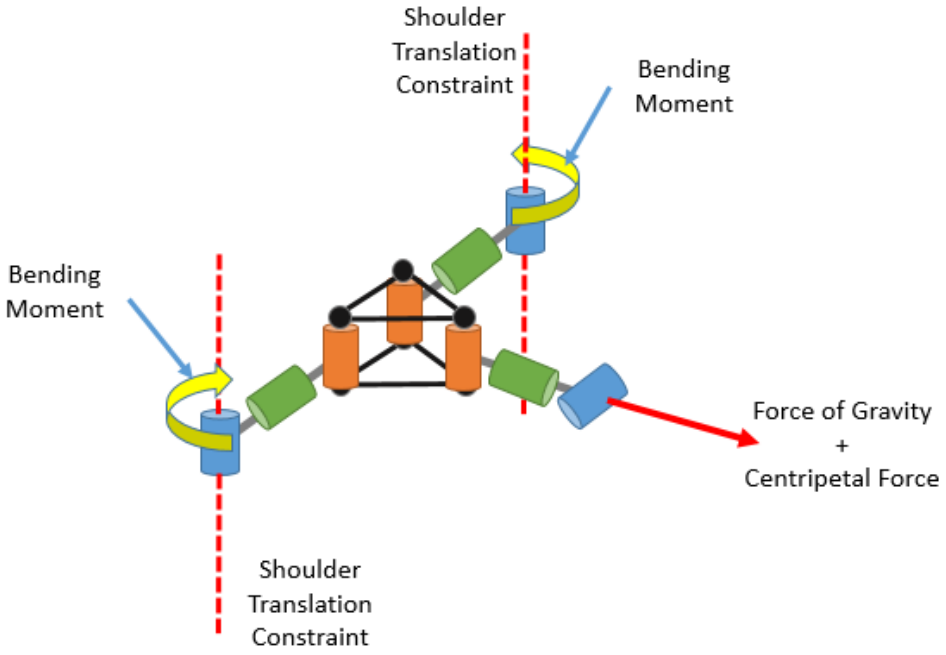

Figure 44 – FEA Configuration 2

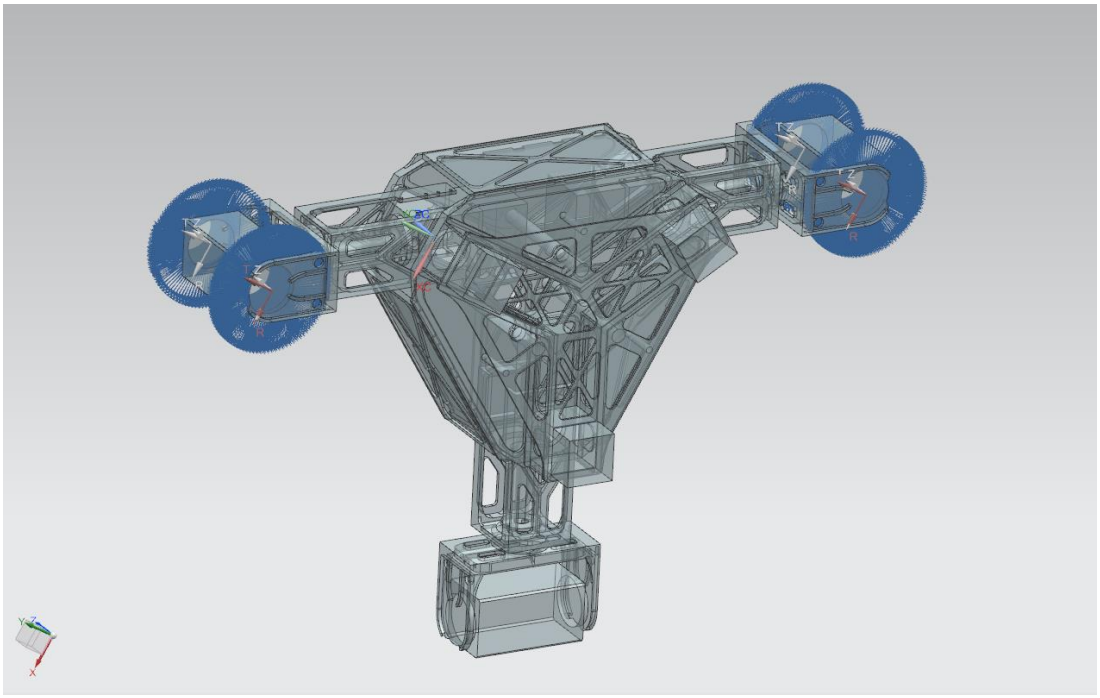

Figure 45 - Constraints Rendered in FEA Model of Configuration 2

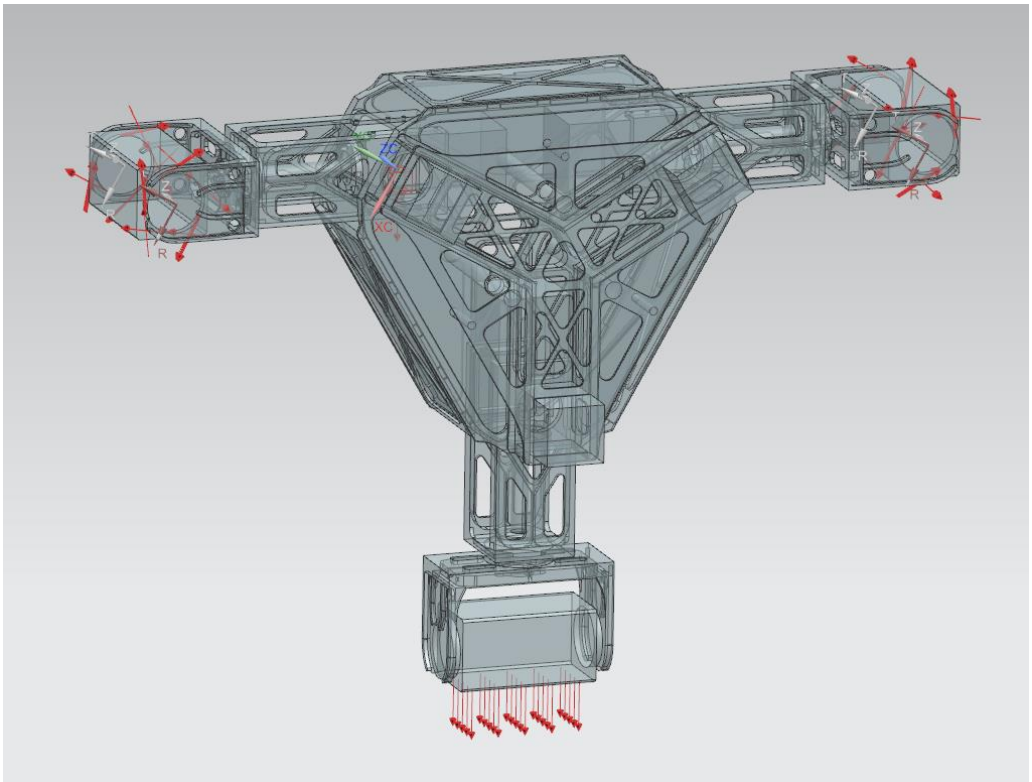

Figure 46 - Loads Rendered in FEA Model of Configuration 2

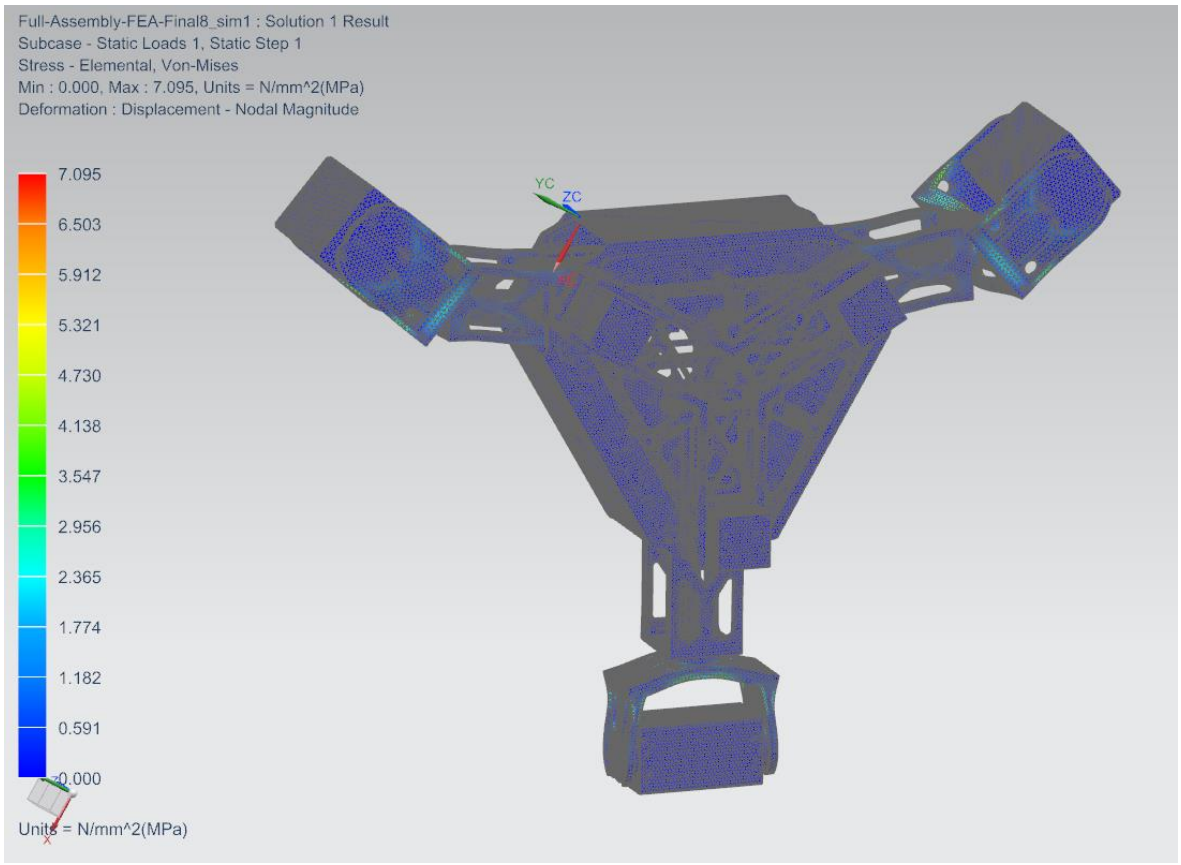

Figure 47 – Resultant Stresses for Configuration 2

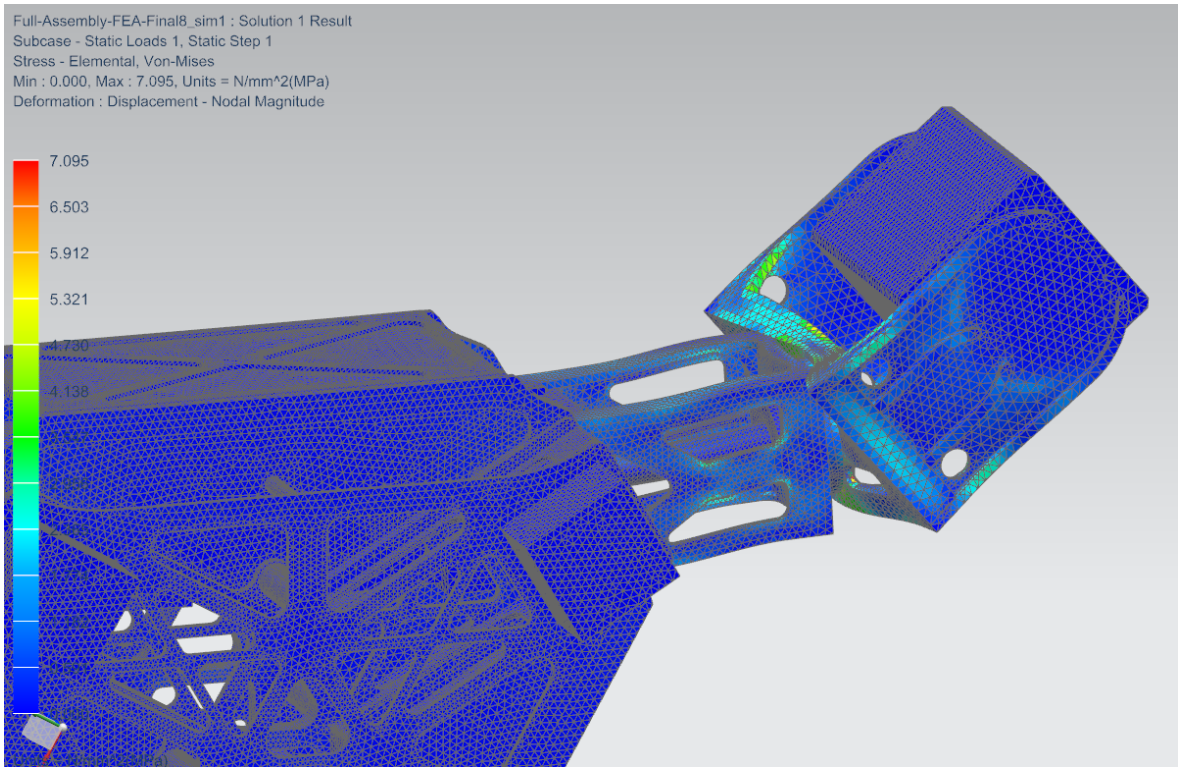

Figure 48 – Detailed View of Resultant Stresses in Configuration 2

2.4.2.3 FINITE ELEMENT ANALYSIS RESULTS

In both configurations the resulting stresses and deflections were minimal and are summarized below in table 4.

Table 4 – Summary of FEA Analysis

	Configuration 1	**Configuration 2**
Max Stress	0.1174 MPa	7.095 MPa
Max Deflection	0.0007 mm	0.05 mm

2.5 LEG DESIGN

The leg of the THALeR Platform is the last to be designed because its design does not necessarily depend greatly on the size or shape of the upper body and shoulder assemblies. The leg only needs to be strong enough to support the weight of the system either standing on all three legs or just two. The leg houses a single degree of freedom at the knee pitch joint. In the motor sizing section it was decided that a 100W actuator needed to be used due to the power limitations of the slip ring. The design of the knee actuator assembly and the legs themselves will be very simple. We will start with the selection of appropriately sized carbon fiber tubes which will make up the majority of the leg assembly.

Carbon fiber was chosen for its extremely high strength to weight ratio. In addition our lab has a wealth of previous knowledge and experience working with the material. The carbon fiber tubes were selected to give appropriate strength and stiffness to support the body of the robot. However the carbon fiber tubes should not be too stiff because the impact forces of the swing leg hitting the ground are quite large and we would like to absorb some of that energy in the bending of the tubes themselves. This will prevent some of the impact loading entering directly into the gear trains of the actuators. It is very difficult to accurately predict the exact energy absorbing capabilities of different tube cross sections and lengths. In order to account for this unknown the leg assembly was designed to be as modular as possible. Therefore, if it was discovered later that the chosen tube cross section was over or under-sized for the application, only the individual tube sections and adapters would have to be replaced without replacing the rest of the assembly that affixes to the actuators themselves. In addition the lab already had a small stock of numerous sizes of carbon fiber tubes one of which was estimated to be an appropriate size for the leg assembly. There was nearly enough tube material to manufacture half of the legs needed which greatly reduced the overall cost for completing the platform. This cost saving was a large motivation for choosing a tube size that was already in stock. The final tube size was 0.87” outer diameter by 0.75” inner diameter.

The rest of the leg design proceeded by creating adaptable brackets for each connection point that would be sufficiently simple to manufacture while limiting weight and providing adequate strength. The final leg design can be seen in figures 49 and 50.

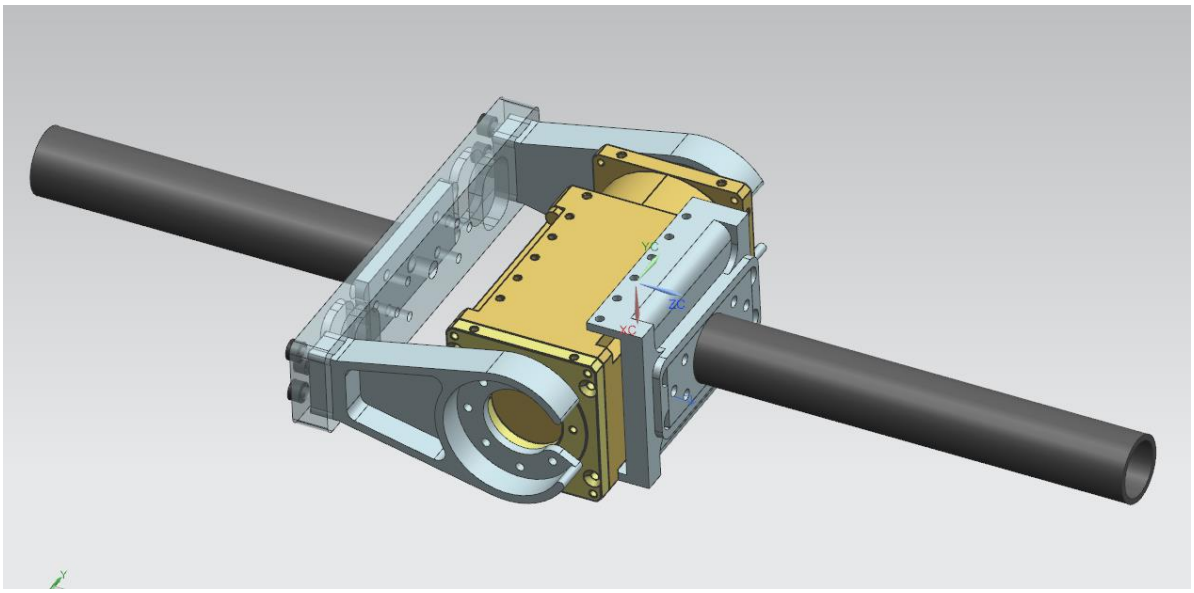

Figure 49 – CAD Model of Modular Knee Assembly (Front View)

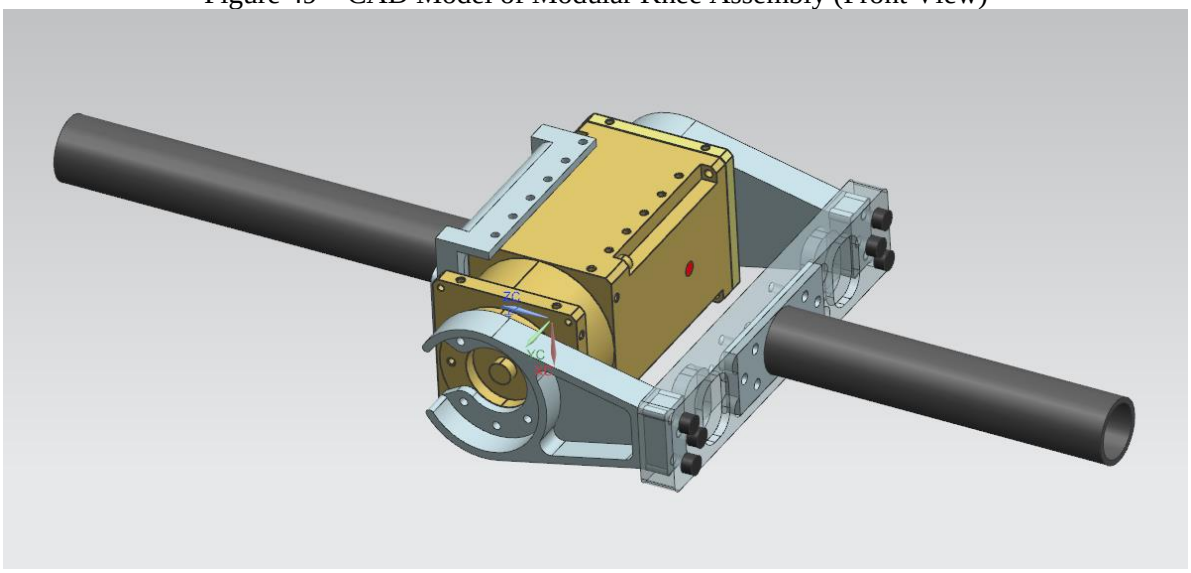

Figure 50 – CAD Model of Modular Knee Assembly (Back View)

3 SWING-THROUGH GAIT DESIGN

3.1 SIMPLIFICATION OF THE SYSTEM

Prior to discussing gait strategies in any further detail, the three dimensional model of the system can be greatly simplified. This is done not only to more easily visualize differences in gait strategies but will also be used later to develop a balance controller for the system. As seen in figure 51, the complete three dimensional system consist of a body link with three legs. The model can be greatly simplified however since many of the actuated joints of the system are only used to orient the robot into a "ready to step" state shown in figure 51. Once in this state, many of the joints used for orienting are effectively locked out until the step is completed. In order to enter the ready to step state the most important action is the hip roll axis of both stance legs are aligned with one another to form a rigid axis about which the entire body of the robot can swing (figure 1). Once this occurs, all the actuators in the stance legs are locked out with the exception of the hip roll. In addition the swing leg should ideally rotate straight through both stance legs meaning the hip yaw and roll axis of the swing leg should also be locked out. This means that during the swing phase only 4 of the entire 12 actuated degrees of freedom are used. In addition two of these four degrees of freedom (each stance leg roll actuator) are collinearly located and oriented which implies they can effectively be combined into a single degree of freedom. This brings the system to 3 actuated degrees of freedom; swing leg hip pitch, swing leg knee pitch, and stance leg hip roll. Finally one can notice that all the remaining degrees of freedom are oriented in the same direction with an axis normal to the plane bisecting the stance legs and containing the swing leg. This means the entire 12 DOF, 3D system can be converted into a planar 3 DOF system with an un-actuated foot joint. The final simplified system can be seen in figure 52.

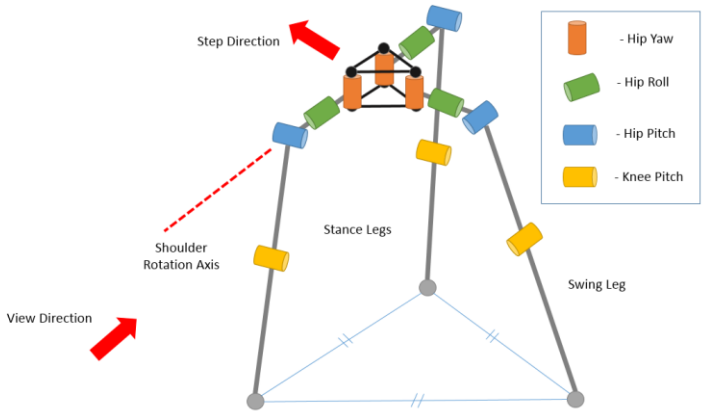

Figure 51 – Figure showing the transformation from a 3D model to a 2D planar model. 3D model should be viewed from the left side while walking the robot walk from right to left.

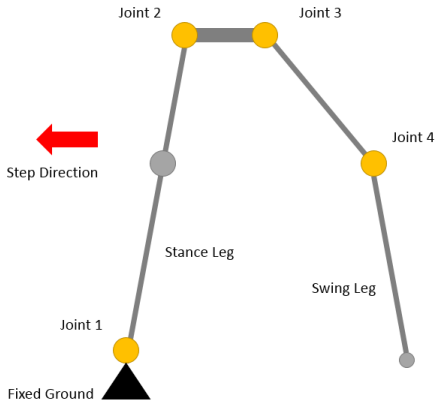

Figure 52 – Simplified 4 DOF Planar System

3.2 NOVEL GAIT METHODOLOGY

The THALeR Platform has undergone numerous iterations. There have been multiple different attempts made at generating a reliable and repeatable open-loop gait strategy for each platform. Although numerous different methods of derivation and optimization of gaits were explored, none were able to be implemented repeatably on hardware. In all the research that has been completed over the years there is one assumption that never changed; the taller the system is, the easier it should be to take a step. This is based on the observation that the taller the platform is the longer the time constant of the inverted

pendulum system is, therefore the system has more time to take a step. This should theoretically make it easier to take a complete step. Since no system has ever been made near the height of the current system it was decided to initially continue with an open-loop gait strategy similar to previous methods.

Although an open-loop strategy (swing through gait) is going to be pursued we will not continue with the exact same gait structure as previous iterations. By "structure" I mean the method in which the gait is executed to increase robustness. The basic gait structure used previously is shown below in figure 53.

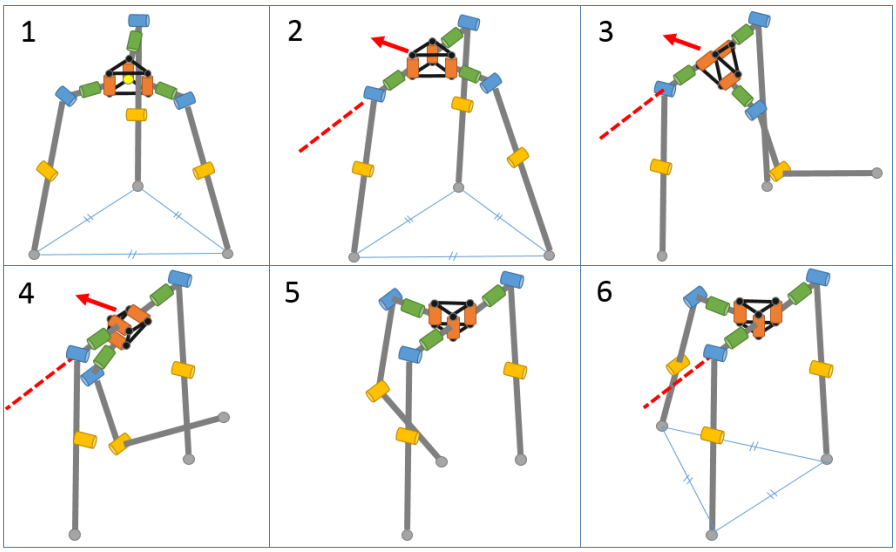

Figure 53 – Overview of Swing Through Gait Methodology

In reading through previous research and watching videos of previous gait attempts, there were a number of theoretical fundamental flaws that were observed which could be improved upon. There were two main considerations in particular. The first consideration regards the method in which the step is initiated which involved slowly tipping the system over until it started to fall naturally. As soon as the fall was initiated this would trigger the lifting of the swing leg to clear the ground and attempting to pass the swing leg through the stance legs fast enough before the system actually fell over. This means the time in which the system has to recover is limited to the fall time from the starting of the tipping point, defined as the point when the center of gravity of the entire system passes the line connecting the two stance feet, to the touchdown point when the swing foot touches the ground again. This recovery time can be increased by implementing a push-off. The push-off should ideally be tuned so that the system has minimal velocity when reaching the tipping point. If implemented successfully the allowable step time can be increased from the previous method (tipping point to touchdown) to include the time from the point where the swing foot leaves the ground to the tipping point. Previously these two points would occur simultaneously. Adding a push-off increases the time between the liftoff point and the tipping point. This concept is illustrated below in figures 54 and 55.

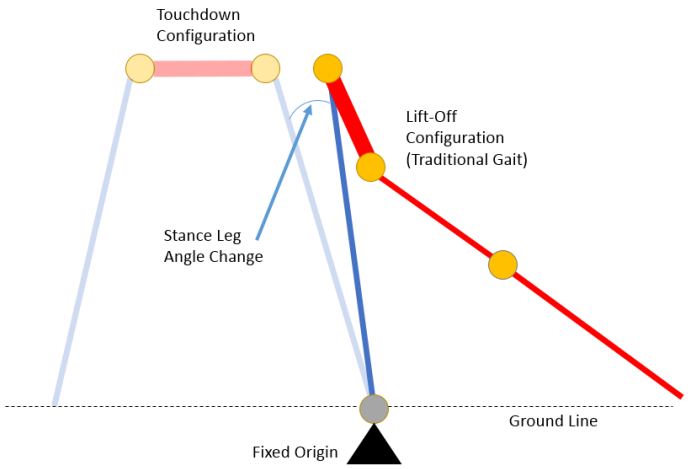

Figure 54 –Stance Leg Angle Deviation During Step Using Traditional Gait

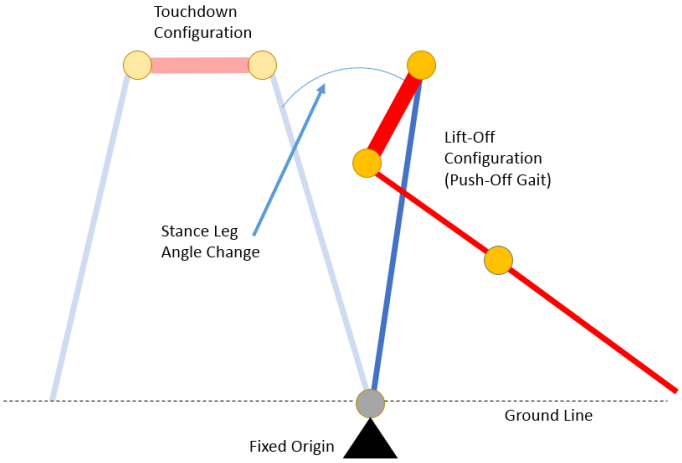

Figure 55 - Stance Leg Angle Deviation During Step Using Push-Off Gait

The second hypothesis to improve gait robustness is reversing the direction of the swing knee during the step. In previous gaits the swing knee was always rotated much like a humans during a step, where the swing knee rotates the swing foot in the direction opposite the direction of the step. This is not ideal in our case for a number of reasons. Firstly, if the system falls more quickly than expected or the swing leg does not move as quickly as expected then the swing foot may not be far enough ahead of the center of gravity of the system when the foot contacts the ground to create a stable landing. The system's momentum will carry the center of gravity of the system over the swing foot contact point causing the system to collapse. By using the previous gait, the foot is rotated farther backward during the step therefore increasing the chances that if the system falls prematurely, that the foot will not be far enough ahead of the center of gravity to actually catch the fall. This can be remedied by having the knee rotated the opposite direction during the step thereby moving the swing foot farther in front of the system's center of gravity and increasing the chances of a stable landing. This concept is demonstrated below in figure 56 and 57.

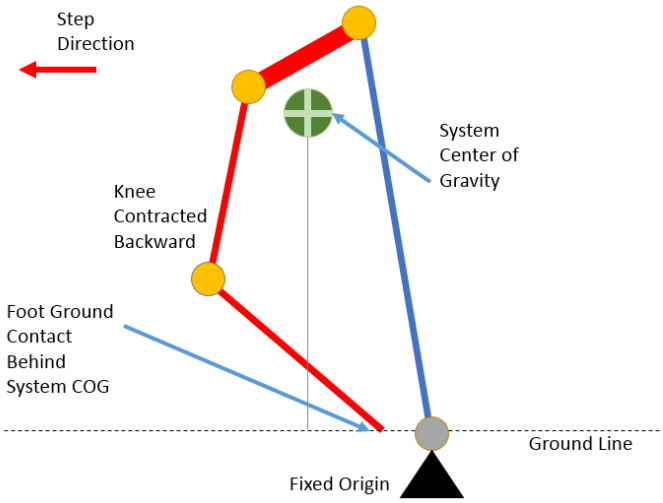

Figure 56 – Premature Foot Ground Contact with Knee Joint Bent Backward During Gait

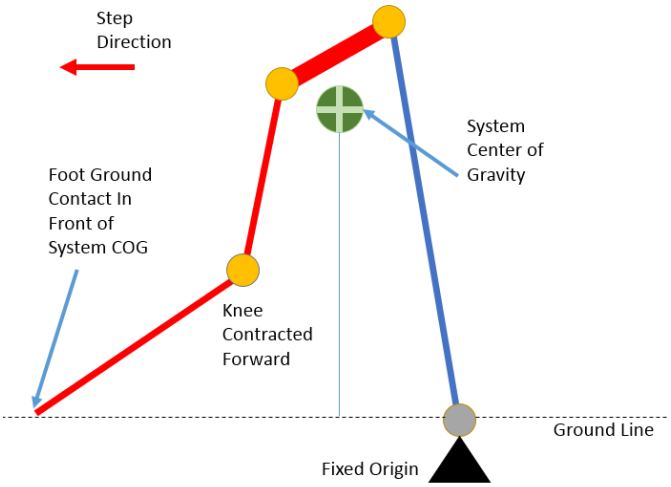

Figure 57 – Premature Foot Ground Contact with Knee Joint Bent Forward During Gait

The second reason for reversing the direction of swing knee rotation during the step is to increase swing foot ground clearance during the step. In the final phase of the step, no matter what direction the swing knee is rotated, the swing leg must be straightened again for a stable touchdown. As the knee is straightened the swing foot moves in an arc about the swing knee. It can be shown that with the upper half of the swing leg in any "near touchdown configuration" the ground clearance during the swing leg straightening process will be greater when the swing foot is being rotated in the direction opposite the gait. This can be shown below in figures 58 and 59.

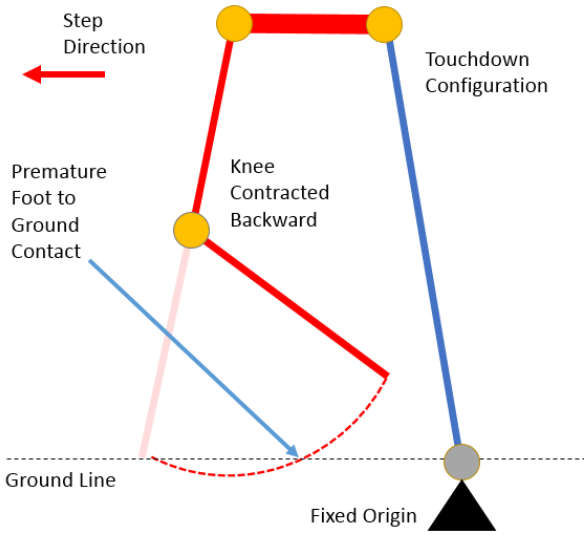

Figure 58 –Swing Foot Ground Clearance During Step with Knee Contacted Backward

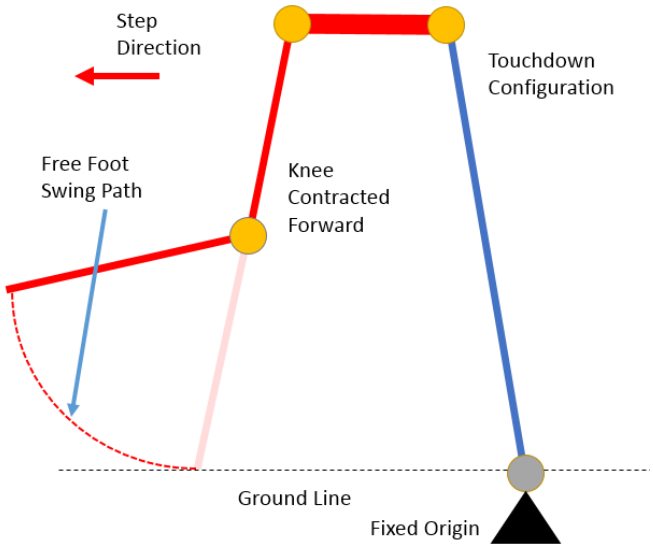

Figure 59 - Swing Foot Ground Clearance During Step with Knee Contacted Forward

With these considerations in mind a theoretically more robust gait is proposed which includes a push-off phase and reversing the direction of swing knee rotation during the step to increase foot placement distance ahead of the center of gravity and to increase swing foot ground clearance during the touchdown phase.

The gait will be further designed using a Matlab graphical user interface, (GUI), initially created by another graduate student Hunter McClelland to quickly adjust time series joint angles and create a cubic spline interpolation between them. In addition an animation of the designed gait can be played back at chosen speed for evaluation. The GUI does not take the system dynamics into consideration when designing the gaits but is instead intended to give the gait designer an intuitive feel for the system in order to determine a small set of parameters that can be tuned in order to develop a final dynamic gait with minimal effort.

The initial layout of the GUI is outlined as follows. It features two interface screens, one to define the system geometry and gait trajectory, and another to view a video playback of the designed gait. On the design screen, time-series joint angles can be input by the user by directly clicking on the joint angle time-series plots for any one of the four controllable joint angles. Note that since system dynamics are not taken into account the user must manually specify the trajectory for joint angle one as well as the three controllable joints 2-4. Points can also be entered more precisely via an input menu where the user can enter joint angles and velocities numerically. The user can also specify the basic geometry of the system such as the height and initial stance dimensions which defines the initial joint angles. The basic layout of the two screens that make up the GUI can be seen below in figures 60 and 61.

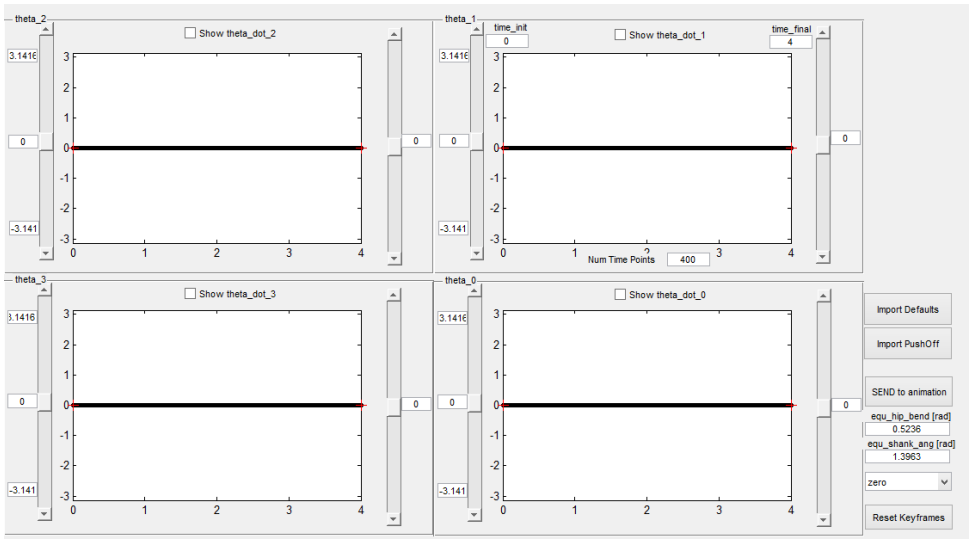

Figure 60 – Matlab Graphical User Interface for Gait Design

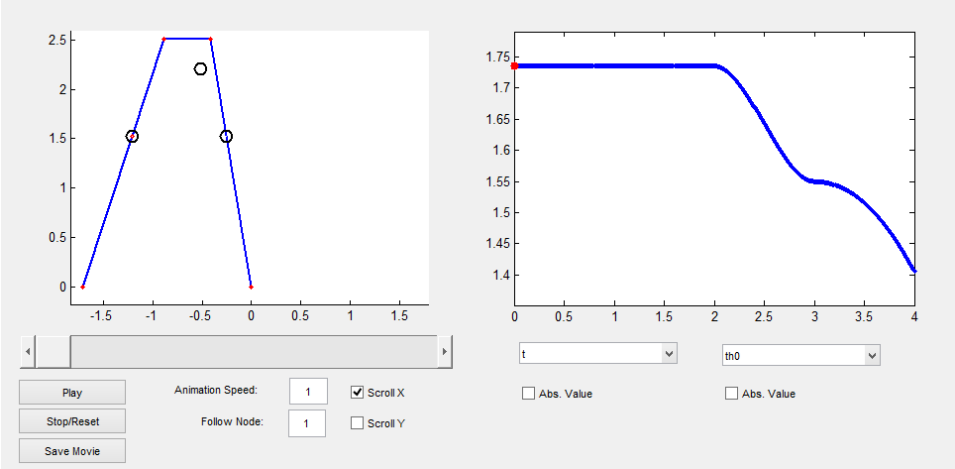

Figure 61 – Matlab Graphical User Interface for Gait Visualization

During initial gait design the Matlab GUI was altered to include features desired during the development process. These features included ability to import pre-saved joint positions and velocities, as well as the ability to solve for "push-off points". This GUI did not originally take into account system constraints such as both feet being in contact with the ground. The user could specify any set of continuous time-series joint positions for all four joint angles with no other stipulations. Since a push-off phase was desired an automatic push-off phase calculator was integrated. This was done by specifying a trajectory for joint angles 1 and 2, and solving for joint angles 3 and 4 with the constraint of the swing foot

remaining in contact with the ground. The push-off phase would automatically end when the swing knee joint reached zero degrees at which point it was assumed the swing foot would leave the ground. With the GUI completed one could very quickly design new gaits and export them for use in simulation software. Again the overall goal of this being two fold;

1. Achieve a successful dynamic gait working in simulation
2. Determine a set of parameters which could be quickly changed during hardware testing to either slightly or significantly alter gait trajectories without using the GUI. This will allow quick turn-around time in testing. The final method for using the GUI is detailed step by step below in figures 62 through 65.

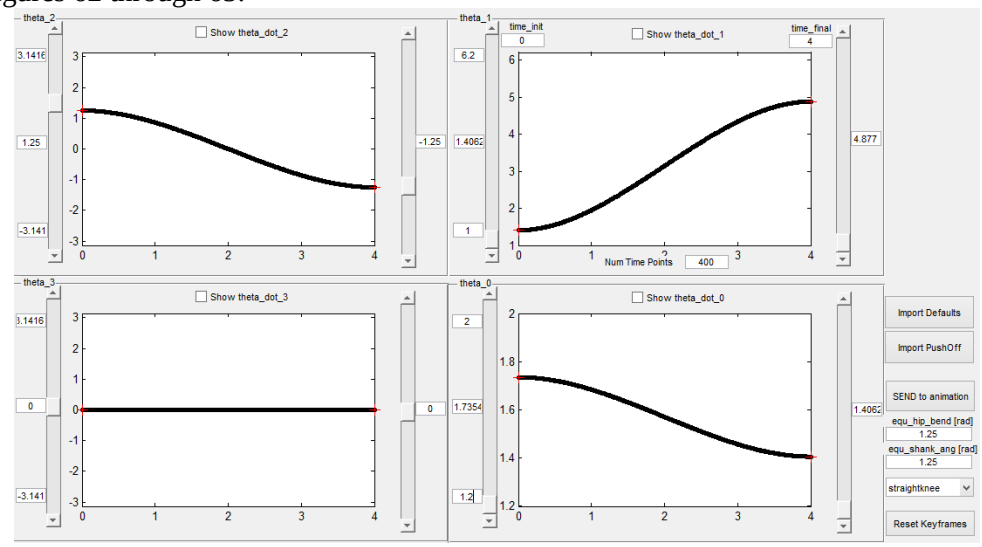

Figure 62 – Trajectory After Inputting Desired Equilateral Stance Geometry

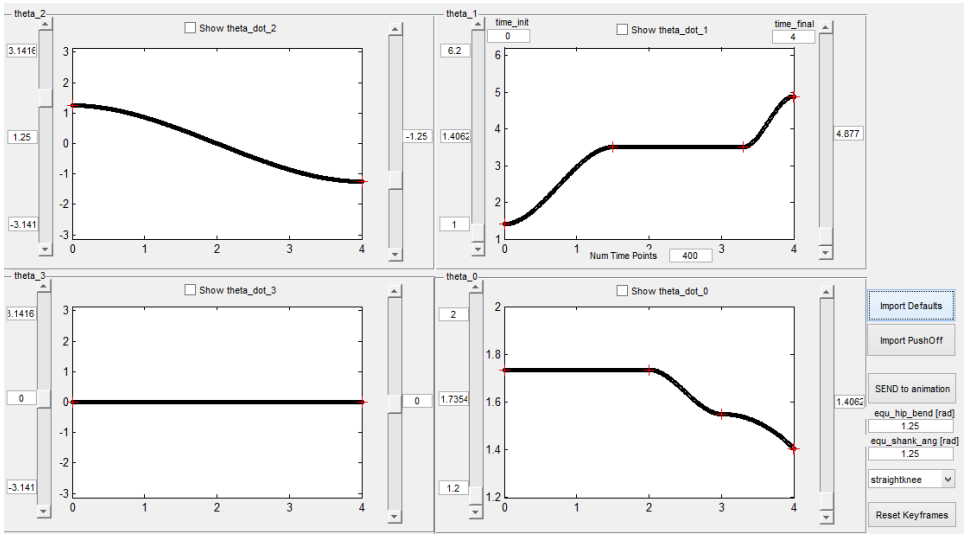

Figure 63 – Trajectory After Inputting Desired Path for Theta 1 and Theta 2

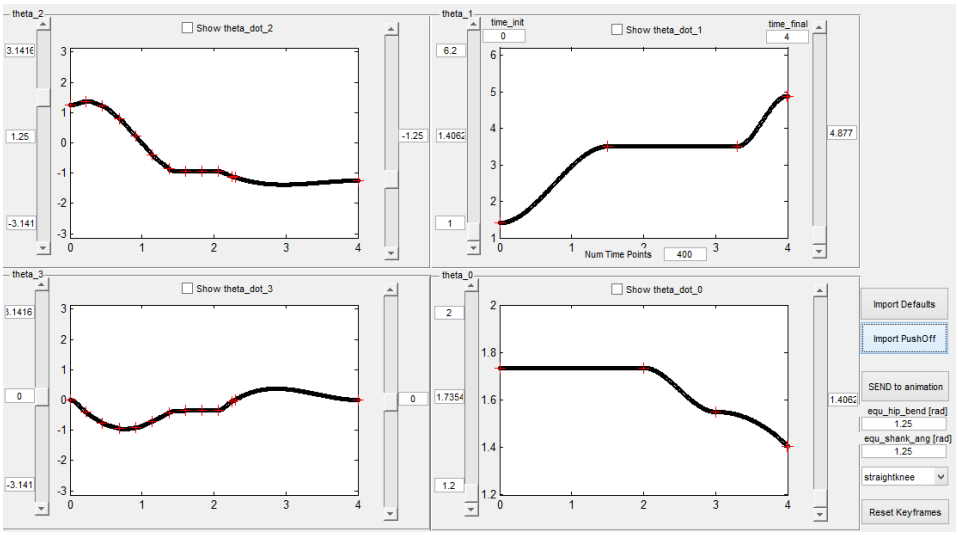

Figure 64 – Trajectory After Automatically Calculating the Push-Off Phase Using Previous Inputs

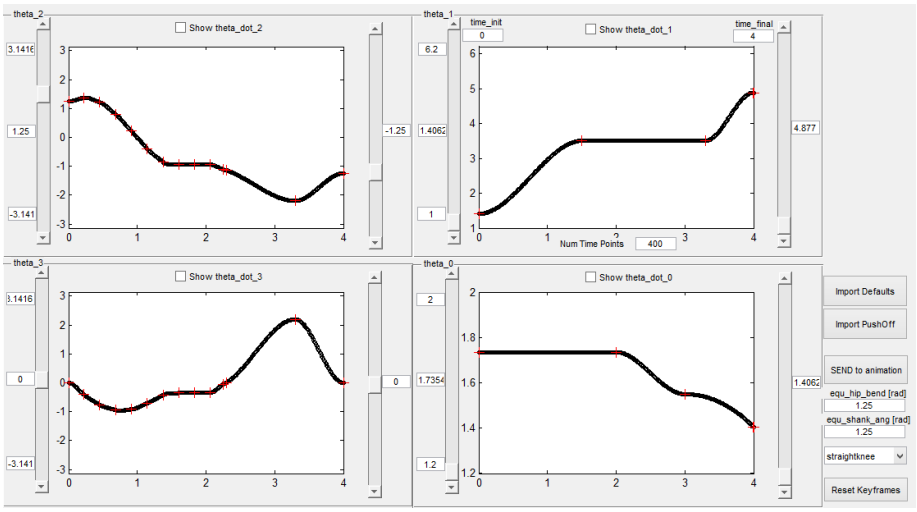

Figure 65 – Trajectory After Manually Adding Trajectory Points to Joints 3 and 4 for Ground Clearance

3.3 SWING THROUGH GAIT SIMULATION

With the GUI Gait Designer completed the next step was to model the system in simulation and start attempting designed gaits. The goal is to design a successful gait in simulation as well as determine a set of parameters that can be quickly tuned on the hardware itself to achieve a successful step.

For simulation purposes an open source software package called Gazebo was used. It allows the generation of simulated physical models using basic geometric building blocks such as boxes and cylinders which can be assigned masses and moments of inertia. An approximate model of the completed THALeR platform was created and is shown in Appendix C. An image of the model in the gazebo environment can be seen below in figure 66.

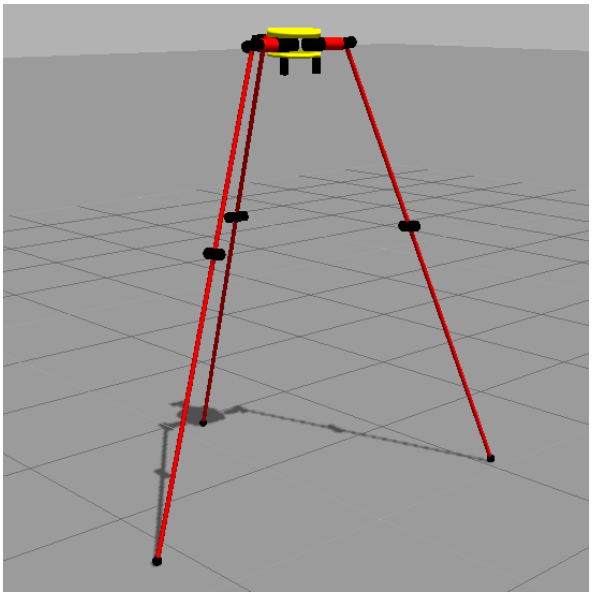

Figure 66 – Gazebo Model of THALeR

In order to control the gazebo model in real-time, an interface between the gazebo framework and the lab's standard control software framework was written by Dr. Michael Hopkins. This interface allows the exact same software framework that will run onboard the robot itself to be used to control the gazebo model. This will allow the simultaneous testing of gait designs in simulation while learning how to work within the framework that will be used on hardware.

With the interface and framework in place gait designs could be very quickly tested. This was a long iterative process where at the end of which a number of successful gaits were designed with varying stance geometries but all using the same gait strategy detailed earlier. More importantly during this process a methodology was developed that allowed for very quick gait generation using system knowledge and a small set of system parameters detailed in the following section.

3.4 SWING THROUGH GAIT PARAMETER SELECTION

Through extensive testing in the previously described simulation environment, many different gaits were generated and evaluated. Through this process a correlation between joint trajectory shapes and dynamic system behavior could be developed through observation. The true correlation lies in the non-linear dynamic equations of the system, however what we were looking for was a quick way to tune the overall gait strategy to suite the hardware platform online using a small number of iterations. This can be done by designating and adjusting the following four parameters;

1. Equilateral Stance Width
2. Joint Angle 2 During Push-off
3. Push-off Velocity
4. Swing Knee Contraction Duration

Next we will briefly describe how these parameters where chosen and where they originated from. Early attempts at creating a repeatable gait in simulation where very difficult. The main challenge was in simultaneously coordinating all joints together to complete every stage of the gait; push-off, swing through, and touchdown. One of the easiest ways to simplify this is to lock out specific joints in particular stages to decrease the available degrees of freedom for tuning. It turned out that by locking out joint 2

during the push-off stage not only made for a more reliable push-off but also allowed the stance and push-off parameters to be more easily tuned. With joint 2 fixed during push-off the only other joints that could be actuated are joints 3 and 4. Finally by assuming that the push-off is completed when joint 4 reaches zero degrees, one can find the exact set of angles for joints 3 and 4 that will transfer the system from a cocked, ready to push-off stance (figure 55), through push-off completion. Therefore in order to completely define the geometry of the system during the push-off phase one only needs to define the stance width and the value for joint angle 2 during push-off.

As previously mentioned the addition of the push-off phase into the gait is required in order to increase the amount of time the system is bi-pedal. This allows more time for the system to reconfigure itself into the touchdown position before falling over and should allow for a more repeatable gait. It is obvious that the lower the systems angular velocity about the stance foot during the step, the more time it will have to complete the step. This angular velocity is not constant but is set in motion by the magnitude of the push-off velocity. Therefore we would like to minimize the push-off velocity in order to maximize step time. However if the push-off velocity is too low the system will not reach its vertical equilibrium point where the system's center of mass is directly above the line connecting the two stance feet. If the center of gravity never crosses this line, the system is going to fall backward instead of forward and the step will never be completed. Therefore, in order to maximize step time the strength of the push-off should be tuned to just barely get the systems combined center of mass to pass the line connecting the stance feet. This is the reasoning for the definition of the third gait adjustment parameter, "push-off velocity".

The push-off velocity was tuned by re-sampling the splined trajectory only during the push-off phase and adjusting the time step to either be executed slower or faster. An algorithm was written to do this either in the GUI or in real-time on the hardware platform itself.

With these three parameters defined, the other two stages of the gait, swing through and touchdown, are practically solved. Once the system is in the swing through state, where the swing foot is no longer touching the ground the only goal is to get the swing leg through the stance legs as quickly as possible without having the swing foot touch the ground prematurely. In addition the touchdown pose is always defined as the mirror pose of straight knee shoulder aligned stance of figure 51. In order to reach this pose without touching the swing foot to the ground, one only needs to contract the swing knee (joint 4) as much as possible while rotating joints 2 and 3 into their final touchdown positions. In order to complete this as quickly as possible, we need to define the points where the knee is fully contracted and the touchdown pose with a cubic spline interpolation between them where joint velocities are as high as possible without going over hardware limits. All of this may sound complicated but is relatively straight-forward in practice with the GUI developed. All of these considerations can be taken care of with a few clicks of the mouse. At the end of this process the gait trajectory can be exported and played back in simulation. If the system never reaches the vertical equilibrium point either the stance width can be narrowed or the push-off velocity can be increased. If the system does not have enough time to recover mid-step, the push-off angle of joint 2 can be increased to decrease the angle it needs to traverse to complete the step. If the swing foot touches the ground mid step then it can be contracted earlier in the gait or extended later in the gait. With the basic gait strategy of inverting the swing knee contraction and locking out joint 2 during push-off, the gait trajectory can be almost completely defined with the four parameters above.

3.5 SWING-THROUGH GAIT HARDWARE TESTING

In previous sections a number of different gaits had been developed that were successful in simulation. However simulation has a major drawback in that it is always "perfect". There are no sources of error unless they are manually introduced. In addition there are many different factors in the system which

remained un-modeled such as joint friction and leg deflection (which was significant). Therefore there was a small chance of a gait that was successfully implemented in simulation to directly working in actual hardware, especially since the gait trajectory is run open loop with no knowledge of system dynamics. This was the reason for developing the parameter selection methodology described earlier. This methodology allowed for the development of a tunable gait using a clearly defined stance geometry that could be transferred to the hardware platform directly. Once on the hardware, the gait could be executed and retuned with a very short turn-around time and without the need to return to the GUI unless the stance geometry is changed.

The exact implementation of this method will now be discussed in more detail. The steps for designing and tuning a gait were executed as follows;

1. Set a stance width
    - This single value defines the entire geometry of the stance both in the equilateral configuration of figure 51 and the shoulder aligned configuration of figure 55.
2. Choose a value for joint 2 during the push-off phase
    - This determines how far the system leans back when ready to push-off. The higher this value the higher the push-off velocity will have to be set later. This also determines how much farther joint 2 has to rotate to complete the gait.
3. Use the GUI to generate the rest of the gait automatically.
    - The GUI calculates the points required for a smooth push-off and can also be used to quickly set the swing knee contraction duration.
4. Export gait trajectory to the hardware platform.
5. Execute gait trajectory as many times as desired.
6. Depending on the outcome, the gait may need to be re-derived from any one of steps 1-4 or the push-off velocity can be adjusted onboard which requires no extra derivation.

Some common failures and examples of appropriate responses are detailed below;

- System falls backward mid-step (system is leaning too far back or push-off is not powerful enough)
    - Decrease value of joint 2 during push-off
    - Increase push-off velocity
    - Narrow stance width
- System falls forward (not enough time to complete step)
    - Increase value of joint 2 during push-off
    - Decrease push-off velocity
    - Widen stance width
- Swing foot contacts ground mid-step.
    - Adjust swing knee contraction duration.
    - Decrease push-off velocity

Hardware testing progressed with the above methodology however many new concerns arose. The most significant of which was actuator reliability. The exact same trajectory could be executed and system behavior would vary drastically. Multiple different causes for this were explored including communication errors and packet loss, data corruption, motor controller issues. All of these possibilities were eliminated except for motor reliability issues. The best guess is that since the actuators were prototypes there could have been a few of irregularities between motors causing sources of error. This left testing not only up to parameter tuning but also a great deal of luck. Hardware testing continued in this fashion until motors started experiencing unrepairable electrical failures. It is unknown what the exact

cause of failure was but the end result was either that the motors would not power on anymore or they would power on but communication could not be established. Unfortunately we ran out of replacement motors to repair the system. In all, four motors broke down. The platform was completely disassembled in order to send the motors to the manufacturer for repair in Korea. It was unknown at the time how long it would take to receive the repaired motors back therefore an interim project was conceived that could support further development of the platform.

3.6 MOTIVATION FOR AN UNDER-ACTUATED BALANCE CONTROLLER

The previously discussed "swing through" gait has proven to be very difficult to accomplish in practice. Over many years and numerous iterations of the tri-pedal 12 DOF platform only a hand full of single steps have every been accomplished and multiple steps have never been accomplished in one testing session. [1-7]

Given the inherent instability of the "swing through" gait previously discussed, another gait was proposed that would enable more controlled walking and possibly footstep planning. The "swing through" gait must be executed very quickly in order to be successful. In addition the step must be executed very precisely in order to place the foot exactly where desired. This has been proven to be very difficult during testing and has therefore made any practical foot step planning almost impossible. It may be desired that the step not be executed so quickly. What if the system could actually balance itself in order to give the swing leg enough time to get into the proper orientation for proper foot placement? With this in mind a "Tai Chi" gait is proposed where the swing leg is used as an actuated pendulum to balance the under-actuated inverted pendulum formed by the body and stance legs.

4 BALANCE CONTROLLER DESIGN OF OVER-SIMPLIFIED SYSTEM TO SHOW FEASABILITY

Before attempting any sort of advanced control techniques or delving into the four degree of freedom planar system, shown in Figure 69, we will first seek to simplify the entire system to that of a two degree of freedom under-actuated pendulum shown in Figure 70. The system is non-actuated between the first link and the base but has a single actuator between the first and second link. This configuration is normally referred to as the "Acrobot" in the controls community and there have been many papers written on the topic of controlling the under-actuated system which very closely resembles the planar model of THALeR. [8-10]

4.1 MODEL SIMPLIFICATION

In order to approximate the THALeR platform as an acrobot system we lock out joints 2 and 3. This allows the actuation of joint 1 to allow the swing leg to actively balance the under-actuated stance leg and body assembly.

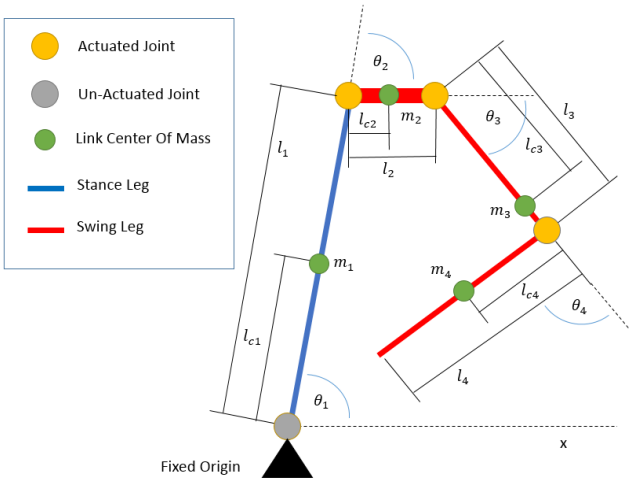

Figure 67 – Reduced Planar System

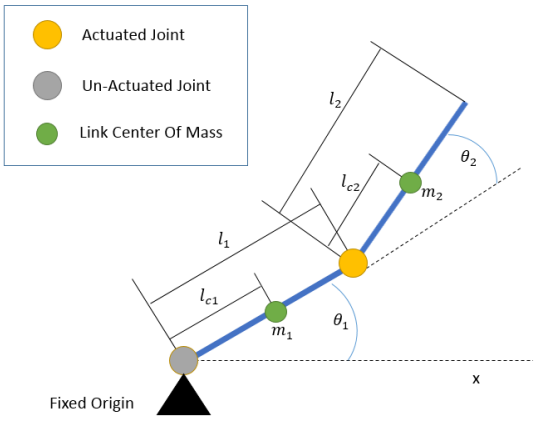

Figure 68 – Equivalent Acrobot Model

The next part of model simplification is to determine the combined positions and magnitudes of the combined center of masses for the simplified system. The acrobot model only has parameters corresponding to links 1 and 2. The full system, however, has masses, mass positions, and rigid body inertias for all 5 bodies that make up the full planar system. The first two bodies which make up the stance leg of the robot need to be combined into link 1 of the acrobot and the last three links which make up the swing leg and body of the full system need to be combined into link 2 of the acrobot model. Using the general equation for combined center of masses along with the parallel axis theorem to combine rigid body inertias the following combined system parameters can be formed from the original system parameters.

Table 5 – Equivalent System Parameters for THALeR and Acrobot								
THALeR System Parameters					**Equivalent Acrobot System Parameters**			
m1	mass of stance leg	1.624	kg		**m1**	mass of stance leg	0.812	kg
m2	mass of body	9.880	kg		**m2**	mass of swing leg	11.032	kg
m3	mass of upper swing leg	0.812	kg					
m4	mass of lower swing leg	0.045			**I1**	Inertia of stance leg	0.1855	$kg \cdot m^2$
					I2	Inertia of swing leg	0.3835	$kg \cdot m^2$
I1	Inertia stance leg	0.0356	$kg \cdot m^2$					
I2	Inertia body	0.8604	$kg \cdot m^2$		**lc1**	length to stance leg com	1.486	m
I3	Inertia of upper swing leg	0.0178	$kg \cdot m^2$		**lc2**	length to swing leg com	0.138	m
I4	Inertia of lower swing leg	0.0086	$kg \cdot m^2$					
					l1	length of stance leg	2.540	m
lc1	length to stance leg com	1.500	m		**l2**	length of swing leg	3.000	m
lc2	length to body com	0.080	m					
lc3	length to upper swing leg com	1.080	m					
lc4	length of lower swing leg com	0.785	m					
l1	length of stance leg	2.540	m					
l2	length of body	0.370	m					
l3	length to upper swing leg	1.080	m					
l4	length of lower swing leg	1.570	m					

4.2 DERIVATION OF EQUATIONS OF MOTION FOR SIMPLIFIED SYSTEM

Using the simplified model of the acrobat, the partial differential equations governing the system dynamics can be derived using first principles using the Lagrange Method [8-10]. The derivation starts by finding the position vectors of the system's two centers of masses ($r_{m1}\ and\ r_{m2}$) and finding the lagrangian "T". All symbols are defined in Table 5 and figure 70.

Define the unit norm direction vectors of each link. [8-10]

$$\alpha(\theta,t) \equiv \begin{bmatrix}\cos(\theta_1(t))\\ \sin(\theta_1(t))\end{bmatrix}$$

$$\beta(\theta,t) \equiv \begin{bmatrix}\cos(\theta_1(t)+\theta_2(t))\\ \sin(\theta_1(t)+\theta_2(t))\end{bmatrix} \quad (9)$$

$$\gamma(\theta,t) \equiv \begin{bmatrix}\cos(\theta_1(t)+\theta_2(t)+\theta_3(t))\\ \sin(\theta_1(t)+\theta_2(t)+\theta_3(t))\end{bmatrix}$$

$$\delta(\theta,t) \equiv \begin{bmatrix}\cos\big(\theta_1(t)+\theta_2(t)+\theta_3(t)+\theta_4(t)\big)\\ \sin\big(\theta_1(t)+\theta_2(t)+\theta_3(t)+\theta_4(t)\big)\end{bmatrix}$$

Now define the position vectors of each link center of mass;

$$\begin{gathered} r_{m1}(\theta,t) = l_{c1}\alpha(\theta,t) \\ r_{m2}(\theta,t) = l_1\alpha(\theta,t) + l_{c2}\beta(\theta,t) \\ r_{m3}(\theta,t) = l_1\alpha(\theta,t) + l_2\beta(\theta,t) + l_{c3}\gamma(\theta,t) \\ r_{m4}(\theta,t) = l_1\alpha(\theta,t) + l_2\beta(\theta,t) + l_3\gamma(\theta,t) + l_{c4}\delta(\theta,t) \end{gathered} \tag{10}$$

Find the velocities of the center of masses;

$$\dot{r}_{m1} = \frac{\partial(r_{mi}(\theta,t))}{\partial t} \quad i = 1 \dots 4 \tag{11}$$

Find the total kinetic energy;

$$T\big(\dot{\theta},\theta,t\big) = \frac{1}{2}\sum_{1}^{4} m_i\|\dot{r}_{m1}\|^2 + \frac{1}{2}\sum_{1}^{4} I_i{\dot{\theta}_\iota}^2 \tag{12}$$

Where I_i is the angular moment of inertia of link i and $\dot{\theta}_\iota$ is the angular velocity of link i. Now define $r_{mi}(2^*)$ as the second row element of vector r_{mi} and find the total potential energy as follows;

$$V(\theta,t) = \sum_{1}^{2} g(m_i r_{mi}(2^*)) \tag{13}$$

Form the Lagrangian;

$$L(\dot{\theta},\theta,t) \equiv T(\dot{\theta},\theta,t) - V(\theta,t) \tag{14}$$

Finally the equations of motion can be derived as follows;

$$\begin{gathered} Eq_1(\ddot{\theta},\dot{\theta},\theta,t) = \frac{\partial}{\partial t}\left(\frac{\partial L}{\partial \dot{\theta}_1}\right) - \left(\frac{\partial L}{\partial \theta_1}\right) = 0 \\ Eq_2(\ddot{\theta},\dot{\theta},\theta,t) = \frac{\partial}{\partial t}\left(\frac{\partial L}{\partial \dot{\theta}_2}\right) - \left(\frac{\partial L}{\partial \theta_2}\right) = \tau_2 \end{gathered} \tag{15}$$

$$\begin{gathered} Eq_1 = \frac{\partial}{\partial t}\left(\frac{\partial L}{\partial \dot{\theta}_0}\right) - \left(\frac{\partial L}{\partial \theta_0}\right) = f_{11}\ddot{\theta}_0 + f_{21}\ddot{\theta}_1 + g_1 + h_1 = 0 \\ Eq_2 = \frac{\partial}{\partial t}\left(\frac{\partial L}{\partial \dot{\theta}_1}\right) - \left(\frac{\partial L}{\partial \theta_1}\right) = f_{21}\ddot{\theta}_0 + f_{22}\ddot{\theta}_1 + g_2 + h_2 = \tau \end{gathered} \tag{16}$$

The parameters above are detailed as follows;

$$
\begin{aligned}
f_{11} &= m_1 {l_{c1}}^2 + m_2\left({l_1}^2 + {l_{c2}}^2 + 2 l_1 l_{c2} \cos\theta_1\right) + I_1 + I_2 \\
f_{12} &= m_2\left({l_{c2}}^2 + l_1 l_{c2} \cos\theta_1\right) + I_2 \\
f_{21} &= m_2\left({l_{c2}}^2 + l_1 l_{c2} \cos\theta_1\right) + I_2 \\
f_{22} &= m_2 {l_{c2}}^2 + I_2 \\
g_1 &= -m_2 l_1 l_{c2} \sin\theta_1 \left({\dot{\theta_1}}^2 + \dot{\theta_0}\dot{\theta_1}\right) \\
g_2 &= m_2 l_1 l_{c2} \sin\theta_1 {\dot{\theta_0}}^2 \\
h_1 &= g \cos\theta_0 \left(m_1 l_{c1} + m_2 l_1\right) + m_2 l_{c2} g \cos(\theta_0 + \theta_1) \\
h_2 &= m_2 l_{c2} g \cos(\theta_0 + \theta_1)
\end{aligned}
\tag{17}
$$

4.3 DETERMINING A MANIFOLD OF BALANCE POINTS

In order to proceed further the non-linear system dynamics need to be linearized about an operating point. For the purposes of this study we want to linearize about vertical balance points for the system. These are points where the combined center of gravity for the system is above the base joint. From here on these points will be referred to as "balance points". These balance points can be found by finding the average center of mass of the system in the "x" direction and equating it to be zero, i.e. above the origin.

$$
m_1 l_{c1} \cos\theta_0 + m_2 (l_1 \cos\theta_0 + l_{c2} \cos(\theta_0 + \theta_1)) = 0 \tag{18}
$$

This equation yields three distinct balance manifolds.

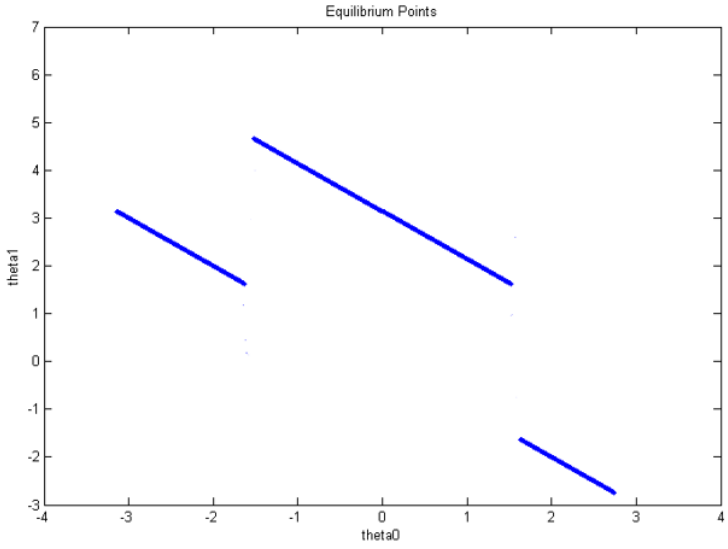

Figure 69 – Balance Manifolds of Acrobot with THALeR Equivalent Parameters

These three manifolds correspond to three distinct families of link orientations.

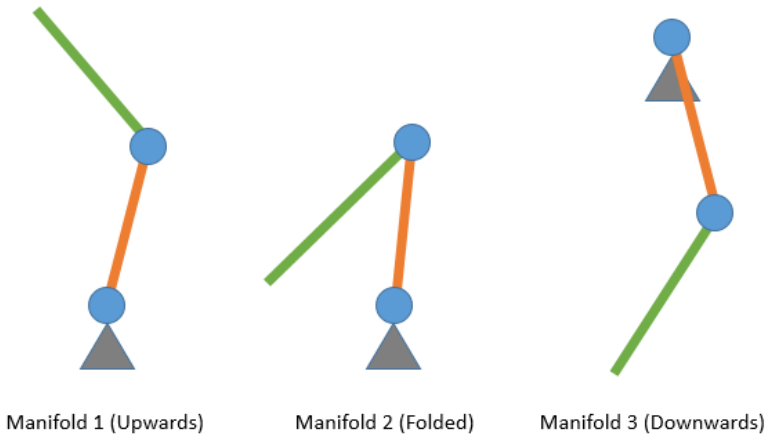

Figure 70 – Geometric Representation of Balance Manifolds

Although these three manifolds exist we are only interested in the one that resembles the geometry of THALeR during a step. This is manifold number 2 above (Folded) where the first link is pointed vertical upwards and the second link is pointed vertical downwards. The first link corresponding to the stance leg of THALeR and the second link corresponding to the swing leg. Around this manifold there are an infinite number of unique balance points. For the purposes of this study we will only proceed with the simplest of possible solutions corresponding to $\theta_0 = {}^{\pi}/_{2}$ and $\theta_1 = \pi$.

4.4 CONTROL OF SIMPLIFIED SYSTEM USING AN LQR CONTROLLER

Now that an operating point has been chosen we can proceed with linearization and control. From before we had;

$$\begin{aligned} Eq_1 &= f_{11}\ddot{\theta}_0 + f_{21}\ddot{\theta}_1 + g_1 + h_1 = 0 \\ Eq_2 &= f_{21}\ddot{\theta}_0 + f_{22}\ddot{\theta}_1 + g_2 + h_2 = \tau \end{aligned} \tag{19}$$

We can form matrices from the non-linear coefficients of the double dot terms and other non-linear remaining terms.

$$\text{Let} \qquad M \equiv \begin{bmatrix} f_{11} & f_{21} \\ f_{12} & f_{22} \end{bmatrix} \qquad G \equiv \begin{bmatrix} g_1 + h_1 \\ g_2 + h_2 \end{bmatrix} \tag{20}$$

We can now solve for the double dot terms and form a set of non-linear ODE's to be linearized.

$$F = \begin{bmatrix} \ddot{\theta}_0 \\ \ddot{\theta}_1 \end{bmatrix} = -M^{-1}G + M^{-1}\begin{bmatrix} 0 \\ \tau \end{bmatrix} = \begin{bmatrix} F_1 \\ F_2 \end{bmatrix} \tag{21}$$

$$\text{Now define the operating point as} \qquad \theta_* = \begin{bmatrix} {}^{\pi}/_{2} \\ \pi \end{bmatrix}, \quad \tau_* = 0 \tag{22}$$

We can proceed with linearizing by forming the Jacobian Matrices that will be used to put the system of equations into expanded state-space form.

$$A_{21} = \left[\begin{matrix} \frac{\partial F_1}{\partial \theta_0} & \frac{\partial F_1}{\partial \theta_1} \\ \frac{\partial F_2}{\partial \theta_0} & \frac{\partial F_2}{\partial \theta_1} \end{matrix}\right]\Bigg|_{\tau_* \theta_*} \quad A_{22} = \left[\begin{matrix} \frac{\partial F_1}{\partial \dot{\theta_0}} & \frac{\partial F_1}{\partial \dot{\theta_1}} \\ \frac{\partial F_2}{\partial \dot{\theta_0}} & \frac{\partial F_2}{\partial \dot{\theta_1}} \end{matrix}\right]\Bigg|_{\tau_* \theta_*} \quad B = \left[\begin{matrix} \frac{\partial F_1}{\partial \tau} & \frac{\partial F_1}{\partial \tau} \\ \frac{\partial F_2}{\partial \tau} & \frac{\partial F_2}{\partial \tau} \end{matrix}\right]\Bigg|_{\tau \theta_*} \tag{23}$$

$$\begin{bmatrix} \dot{\theta_0} \\ \dot{\theta_1} \\ \ddot{\theta_0} \\ \ddot{\theta_1} \end{bmatrix} = \begin{bmatrix} 0 & I_{2x2} \\ A_{21} & A_{22} \end{bmatrix} \begin{bmatrix} \theta_0 \\ \theta_1 \\ \dot{\theta_0} \\ \dot{\theta_1} \end{bmatrix} + [B] \begin{bmatrix} 0 \\ \tau \end{bmatrix} \tag{24}$$

Plugging in all system parameters we obtain the following state space matrices

$$A = \begin{bmatrix} 0 & 0 & 1 & 0 \\ 0 & 0 & 0 & 1 \\ 3.9438 & -2.2201 & 0 & 0 \\ -3.3727 & -39.6475 & 0 & 0 \end{bmatrix} \quad B = \begin{bmatrix} 0 & 0 \\ 0 & 0 \\ 0 & 0.1164 \\ 0 & 2.3162 \end{bmatrix} \tag{25}$$

Finally we can attempt to control the linear system using the LQR method which takes the linearized A and B state matrices along with weighting matrices Q and R and returns an optimized gain matrix G . This G matrix when used as a closed loop feedback gain should render the system stable as long as an appropriate Q and R matrix are chosen. For the purposes of this study we will use the Q and R matrices calculated in for a different acrobot but should still render this system stable.

$$Q = \begin{bmatrix} 1000 & -500 & 0 & 0 \\ -500 & 1000 & 0 & 0 \\ 0 & 0 & 1000 & -500 \\ 0 & 0 & -500 & 1000 \end{bmatrix} \quad R = \begin{bmatrix} 10000 & 0 \\ 0 & 10000 \end{bmatrix} \tag{26}$$

Using Matlab function “lqr” we obtain the following feedback gain matrix.

$$G = [-795.26 \quad 404.6 \quad -3920.4 \quad 0199.1] \tag{27}$$

With the derived controller we can now simulate the full non-linear system with locked out joints to approximate the acrobot while applying the linear control law about the operating point. We start with initial conditions of zero joint velocities and initial joint angles at the operating point plus varying joint offsets at theta0. This produces the following system behaviors which shows the system is rendered stable asymptotically for an initial joint offset less than 0.031 radians. With more time other varied initial conditions could be tested such as non-zero initial velocities and joint offsets on theta1.

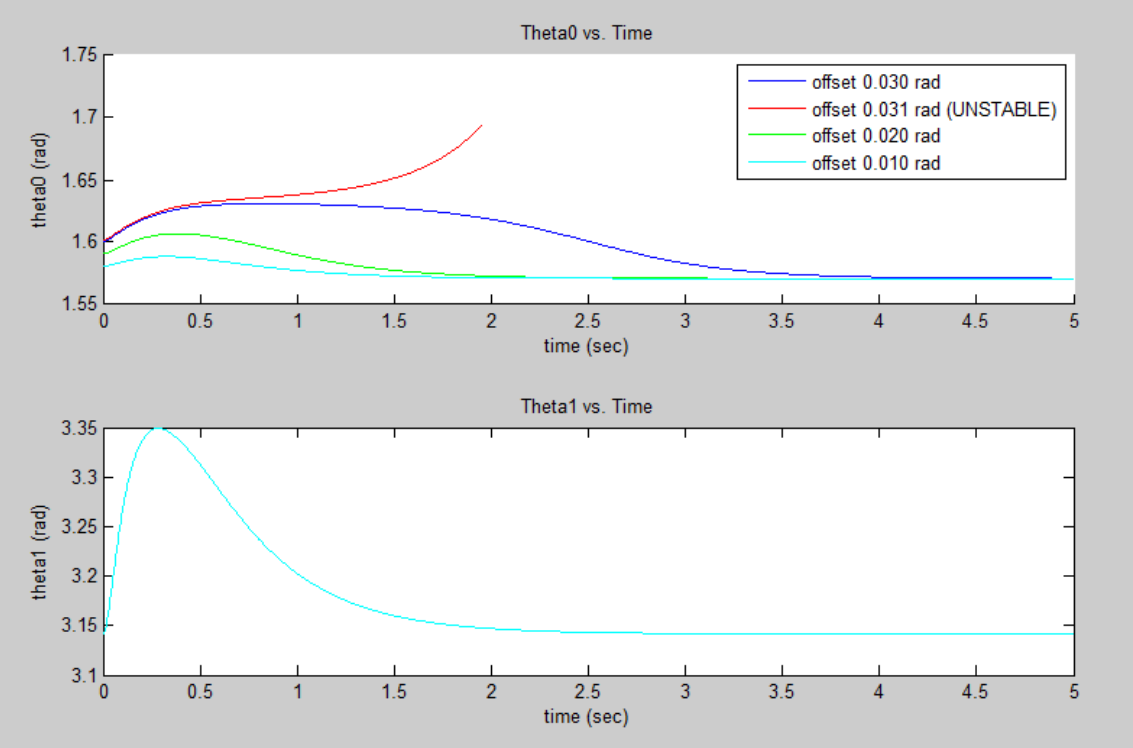

Figure 71 – Time Response of Non-Linear Acrobot System to Varying Initial Conditions

From this we can conclude that the basin of attraction is approximately $\mp 0.03\,radians$ about the operating point, $\left(\frac{\pi}{2}, \pi\right)$. This proves stability for the simplified model and provides a good starting off point for attempting to control the full planer system.

5 BALANCE CONTROLLER DESIGN OF FULL SYSTEM

5.1 BALANCED GAIT DESIGN

The overall goal of the balance controller is to slowly and stably lift the swing leg off the ground, transfer it between the two stance legs to the other side of the body and gently set it down on the ground again in a desired location. During this entire process the whole system acts as an inverted pendulum which is inherently unstable. There does exist, however, a manifold of unstable equilibrium points. Thereforee in order to design a gait one needs to carefully pick a string of equilibrium points that will form a complete step that are all within the equilibrium manifold. Then implement a control strategy to transfer the system through successive equilibrium points.

The first step in designing a possible gait is to define a starting configuration. This initial configuration will be referred to as the "liftoff" pose and can be described geometrically as having the swing leg hip roll axis aligned collinearly with one another, all three stance feet at the points of an equilateral triangle of chosen size in the ground plane and the swing foot applying zero force to the ground (Figure 74). With zero force on the swing foot the combined center of gravity of the system is directly over the line connecting the two stance feet.

In order to find this pose, the feet of the 3D system are set at the corner points of an equilateral triangle of chosen size when the 3D system is viewed from above. This can then be projected into the 2D plane of figure 52 where the distance between the stance foot and swing foot is defined as "sw" or stance width. The swing leg knee joint is set to zero ($\theta_4 = 0$). Now one must derive a set of equations to maintain this geometry and find the unique positions of joints 1, 2 and 3, when the system is quasi-statically balanced on the stance foot. These equations can be derived as follows from the geometric and dynamic constraints of the system in the desired configuration. The coordinate of the swing foot must be located on the ground and a distance *sw* away from the stance foot.

$$\sum_{1}^{4} r_{mi} = \begin{bmatrix} sw \\ 0 \end{bmatrix} \tag{28}$$

Also the average location of the combined center of mass of the system must be directly over the stance foot which we choose as the origin of the system.

$$\sum_{1}^{4} m_i r_{mi}(1^*) = 0 \tag{29}$$

These are three constraint equations then can be used to solve for the three unknown joint angles θ_1, θ_2, θ_3. This solution defines the "liftoff" pose shown in figure 72.

Once the lift-off pose is determined one can proceed to generate the rest of the gate. The gait is designed by choosing a set of intermediary poses that when splined together form a gait with adequate swing foot ground clearance. The first of these poses is the liftoff pose. Since the 2D system is symmetric about the stance foot we do not need to spend time solving for the "touchdown" pose where the robot sets its swing foot back down on the ground. The "touchdown" pose will be the exact mirror of the liftoff pose. One only needs to develop the poses taking the system from the liftoff pose to the touchdown pose while staying in the equilibrium manifold and keeping the swing foot as far off the ground as possible. These poses can be shown in figures 72 through 76.

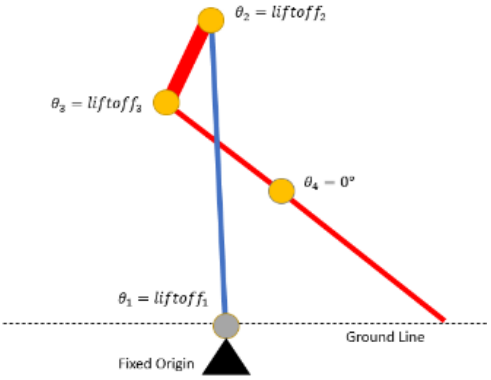

Fig. 72 Pose1 “liftoff”

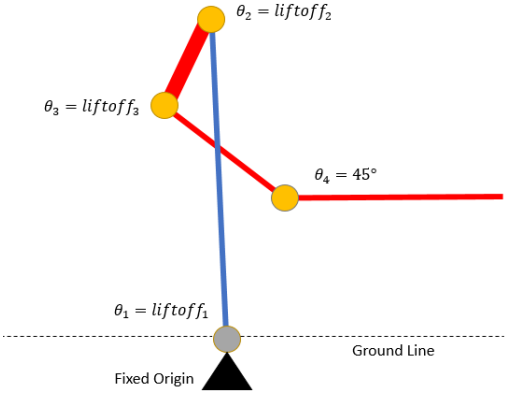

Fig. 73 Pose 2

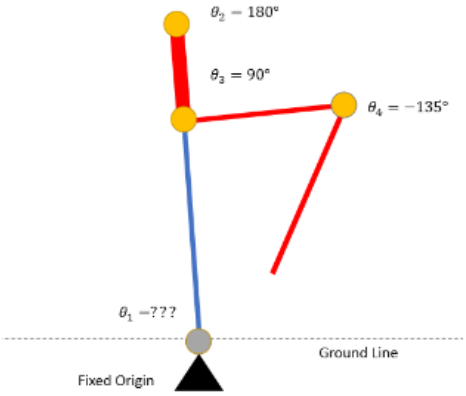

Fig. 74 Pose 3

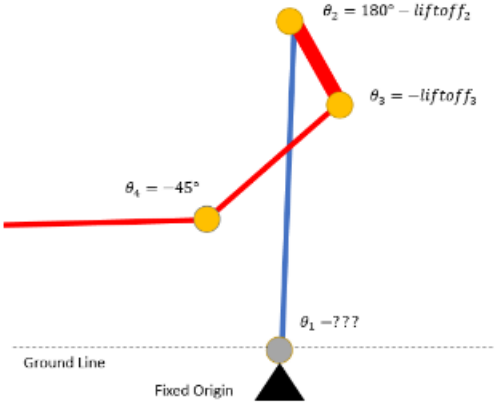

Fig. 75 Pose 4

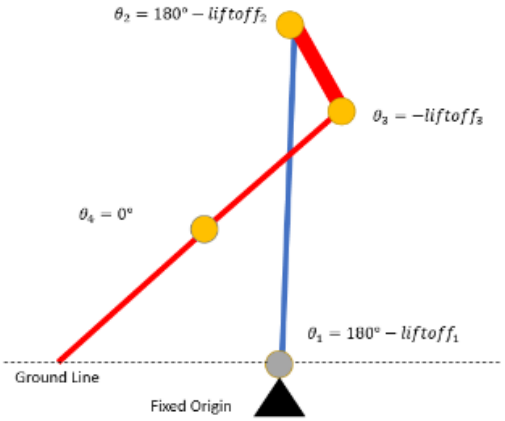

Fig. 76 Pose 5 “touchdown”

Once the intermediary poses have been chosen one can proceed to generate an entire state trajectory of all four joint angles that include the intermediary poses where every state is in quasi-static equilibrium. This is done by generating a fourth order spline connecting each intermediary pose for joint angles θ_2, θ_3 and θ_4, to create a total of $n = 150$ states. Then solving equation 28 for the remaining joint angle θ_1 for all n poses thus guaranteeing each state is an unstable equilibrium. The splined state trajectory can be seen in figure 77.

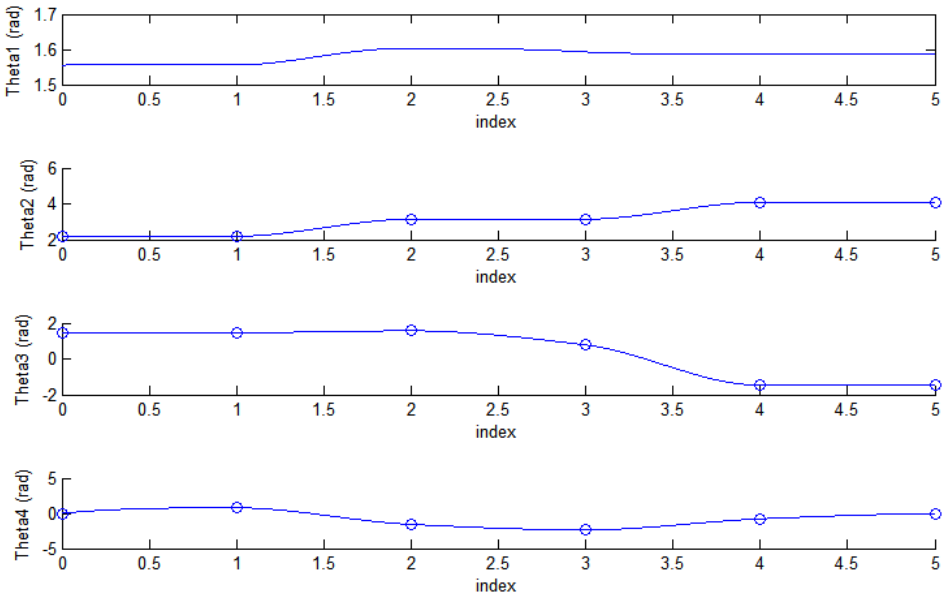

Fig. 77 Balanced State-Space Gait Trajectory

5.2 SYSTEM MODEL

Now that a complete balanced gait trajectory is created we can proceed to develop the controller the 4 DOF planar system. Firstly we must define the system model as follows;

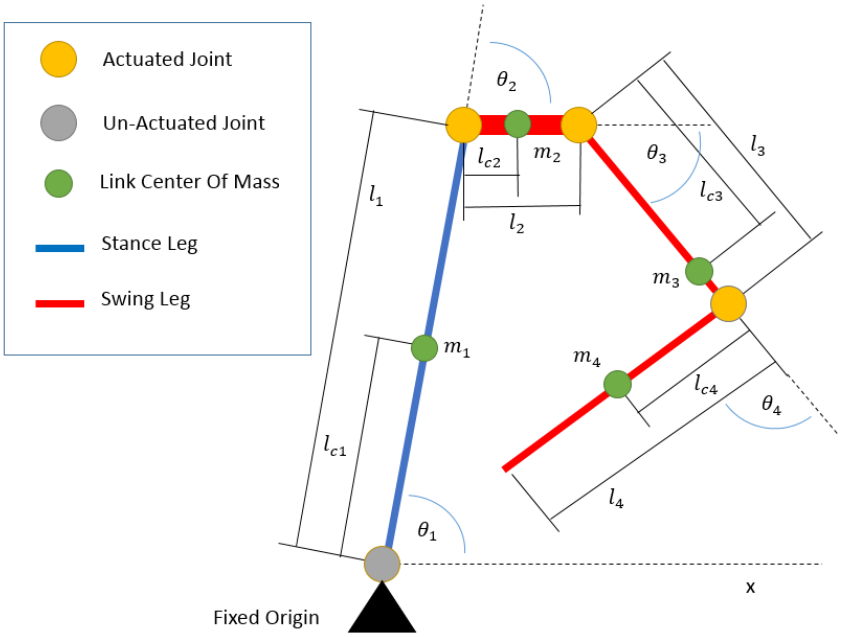

Fig. 78 Simplified Planar System

TABLE 6 – Model Parameter Values

m1	1.624 $\boldsymbol{kg}$	**I1**	0.0356 $\boldsymbol{kg \cdot m^2}$
m2	9.880 kg	**I2**	0.8604 $kg \cdot m^2$
m3	0.812 kg	**I3**	0.0178 $kg \cdot m^2$
m4	0.045 kg	**I4**	0.0086 $kg \cdot m^2$
l1	2.540 m	**lc1**	1.500 m
l2	0.370 m	**lc2**	0.080 m
l3	1.080 m	**lc3**	1.080 m
l4	1.570 m	**lc4**	0.785 m

5.3 SINGLE POINT CONTROLLER DESIGN

A complete gait trajectory has been designed where at each point of the trajectory the system is quasi-statically balanced about the stance foot. The system, however, without a controller is completely unstable about any of these points and therefore a controller must be developed to guarantee convergence about the state trajectory points. For the purposes of this study the controller will be designed using the Linear-Quadratic Regulator (LQR) method to find gain matrices "G_i" that will render the non-linear system stable in a small region around its unique operating point i .

In order to develop the controller the previously derived non-linear system of equations must be put into the proper state-space form to be linearized. It can be shown that equations 7 can be put into the following from ;

$$\begin{aligned} Eq_1 &= f_{11}\ddot{\theta}_1 + f_{21}\ddot{\theta}_2 + f_{31}\ddot{\theta}_3 + f_{41}\ddot{\theta}_4 + h_1 = 0 \\ Eq_2 &= f_{21}\ddot{\theta}_1 + f_{22}\ddot{\theta}_2 + f_{32}\ddot{\theta}_3 + f_{42}\ddot{\theta}_4 + h_2 = \tau_2 \\ Eq_3 &= f_{31}\ddot{\theta}_1 + f_{23}\ddot{\theta}_2 + f_{33}\ddot{\theta}_3 + f_{43}\ddot{\theta}_4 + h_3 = \tau_3 \\ Eq_4 &= f_{41}\ddot{\theta}_1 + f_{24}\ddot{\theta}_2 + f_{34}\ddot{\theta}_3 + f_{44}\ddot{\theta}_4 + h_4 = \tau_4 \end{aligned} \tag{30}$$

Here again the closed form values of these equations are far too long to display in this document so we will continue to work in a symbolic form. These equations can be placed into matrix form as follows

$$M = \begin{bmatrix} f_{11} & f_{21} & f_{31} & f_{41} \\ f_{12} & f_{22} & f_{32} & f_{42} \\ f_{13} & f_{23} & f_{33} & f_{43} \\ f_{14} & f_{24} & f_{34} & f_{44} \end{bmatrix} \qquad H = \begin{bmatrix} h_1 \\ h_2 \\ h_3 \\ h_4 \end{bmatrix} \tag{31}$$

$$\therefore \quad M \begin{bmatrix} \ddot{\theta}_1 \\ \ddot{\theta}_2 \\ \ddot{\theta}_3 \\ \ddot{\theta}_4 \end{bmatrix} + H = \begin{bmatrix} 0 \\ \tau_2 \\ \tau_3 \\ \tau_4 \end{bmatrix} \tag{32}$$

This equation can now be solved for the acceleration vector as follows;

$$F = \begin{bmatrix} \ddot{\theta}_1 \\ \ddot{\theta}_2 \\ \ddot{\theta}_3 \\ \ddot{\theta}_4 \end{bmatrix} = -M^{-1}H + M^{-1}\begin{bmatrix} 0 \\ \tau_2 \\ \tau_3 \\ \tau_4 \end{bmatrix} \tag{33}$$

This matrix equation can now be linearized by calculating the Jacobian matrices of F and evaluating at every state of the trajectory.

$$N_i = \frac{\partial F}{\partial \theta}\Big|_{\theta_i^*} \qquad K_i = \frac{\partial F}{\partial \dot{\theta}}\Big|_{\theta_i^*} \qquad J_i = \frac{\partial F}{\partial \tau}\Big|_{\theta_i^*} \qquad i = 1 \dots n \tag{34}$$

The set of equations in 13 can then be placed into state-space matrix form by defining the state vector;

$$x = \begin{bmatrix} \theta_1 \\ \theta_2 \\ \theta_3 \\ \theta_4 \\ \dot{\theta}_1 \\ \dot{\theta}_2 \\ \dot{\theta}_3 \\ \dot{\theta}_4 \end{bmatrix} \qquad \dot{x}_\iota = A_{8x8_i}x_i + B_{8x3_i}u_{3x1} \tag{35}$$

$$A_i = \begin{bmatrix} 0_{4x4} & I_{4x4} \\ N_i & K_i \end{bmatrix} \qquad B_i = \begin{bmatrix} 0_{4x3} \\ J_i \end{bmatrix} \qquad i = 1 \dots n \tag{36}$$

Finally the feedback control gains can be determined using the LQR method by choosing the appropriate Q and R Matrices . These matrices where determined experimentally by simulating the system at a single equilibrium state and creating a 6 Nm impulse on the base link and analyzing the response. The final Q and R matrices chosen are as follows;

$$Q_{8x8} = \begin{bmatrix} 80000 & 0 & 0 & & & \\ 0 & \dots & 0 & & 0_{4x4} & \\ 0 & 0 & 80000 & & & \\ & & & 30000 & 0 & 0 \\ & 0_{4x4} & & 0 & \dots & 0 \\ & & & 0 & 0 & 30000 \end{bmatrix} \tag{37}$$

$$R = \begin{bmatrix} 1 & 0 & 0 \\ 0 & 1 & 0 \\ 0 & 0 & 1 \end{bmatrix}$$

The feedback gain matrices can be calculated using a standard LQR approach . These gain matrices are designated as G_i.

Finally the steady state input u_i^* can be calculated at each operating point by evaluating the H matrix from equation 11 at each operating point.

$$u^*{}_i = H|_i \tag{38}$$

5.4 ENERGY BASED GAIN SCHEDULER

The overall goal of the gain scheduled controller is to force the system to track the desired trajectory by applying the following control law; [14-20]

$$u = -G_{k+d}(x - x_{k+d}) + u^*_{k+d} \tag{39}$$

Where x is the current instantaneous state, k is the index of the equilibrium state that the system is currently closest to and d is the index increment to the desired state to be instantaneously tracked. The only challenge that remains is to determine the system parameter in which to use to compute the index jump "d" to produce a smooth and stable gait.

In past studies numerous different fuzzy logic approaches have been proposed to choose the method in which to determine a parameter about which to gain schedule [14-22]. For this particular system there are a number of important factors to consider when developing this type of gain scheduling.

1. The system is under-actuated therefore any excessive buildup of angular momentum in the links will result in instability, however one still wants to complete the trajectory in the shortest time possible.
2. The system entirely consists of rotating links. These links require energy input or torque in order to lift them. In addition since there is no damping in the system they require no energy to be rotated back down.
3. A higher index jump “d” produces a higher instantaneous joint torque and similarly a lower or even negative index jump produces a lower joint torque.
4. If the system attempts to reach a point too far ahead in the trajectory that point could be outside of the region of attraction and the system will be unable to reach it.
5. If the system attempts to track a point too close to the current state-space point the state error will be so small that in may not produce a sufficient joint torque to actually move the system.

Once these factors are taken into consideration an energy based method is proposed. This method derives from the hypothesis that to traverse the state-space trajectory smoothly the joints should be more or less moving at a constant angular velocity therefore the instantaneous kinetic energy of the system should be approximately equal at all points in time. Therefore, throughout the trajectory only the potential energy is significantly changing. This can be related to the gain scheduler by the fact that in order to increase the potential energy more torque has to be applied to that joint which means the controller must track a point further along in the state trajectory. Similarly if a link is being lowered the potential energy is decreasing and a point closer to the current state needs to be selected to make sure the link does not move too quickly and build up undesirable angular momentum. With this strategy we can proceed to define a general description of the control strategy that will determine the index jump "d" to be used during real time operation.

Firstly we calculate off-line the potential energy at every point in the state-space trajectory. Then we find the minimum and maximum potential energy values and define them as $pmin$ and $pmax$ respectively. For every point of the state trajectory apply the following laws to determine the index jump d.

If the potential energy of the system is instantaneously increasing, apply the following mapping;

$$d = \frac{(p(i) - pmin)(imax - imin)}{(pmax - pmin)} + imin \tag{40}$$

If the potential energy is instantaneously decreasing apply the following mapping;

$$d = \frac{(p(i) - pmin)(dmax - dmin)}{(pmax - pmin)} + dmin \tag{41}$$

Here the values for $imax, imin, dmax,$ and $dmin$ are minimum and maximum index jump values for the gain scheduler. They are chosen to provide adequate gait completion speed while not going to fast as to build up excessive inertia or be unable to reject disturbances. For the system in question these values were chosen to be;

$$\begin{matrix} imax = 160 & dmax = 100 \\ imin = 80 & dmin = 60 \end{matrix} \tag{42}$$

This mapping can be computed entirely off-line and produces the following graph showing the change in potential energy along with the calculated index jump "d" computed at every index point.

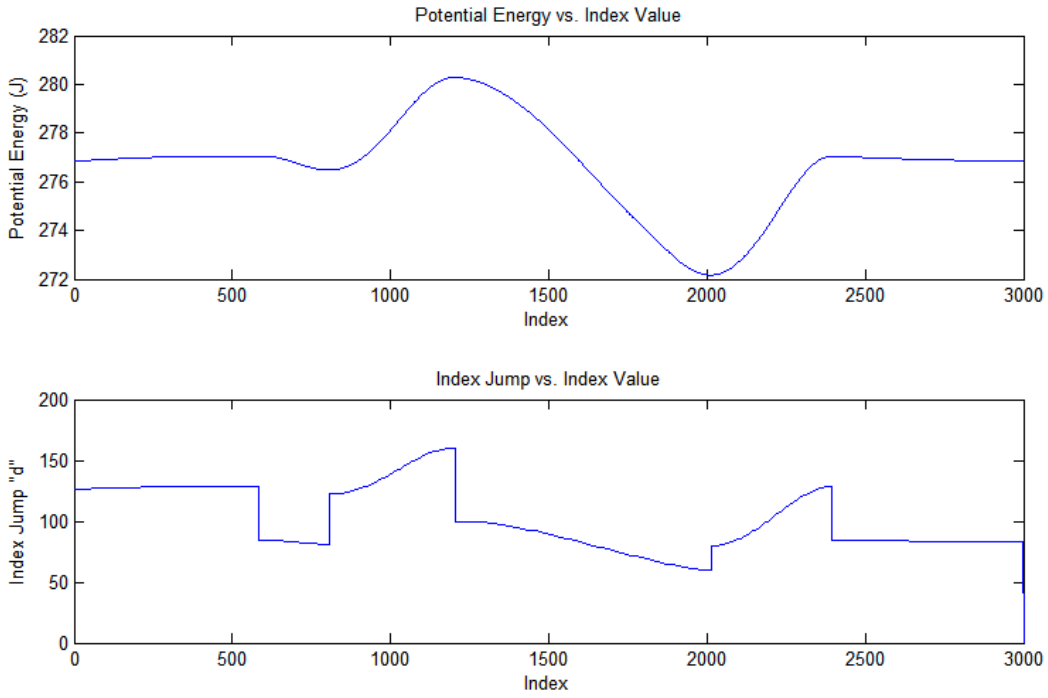

Fig. 79 Potential Energy during Gait and Index Jump Calculated from Equations 19 and 20.

5.5 SIMULATION RESULTS

The 2D non-linear system was modeled in Matlab Simulink SimMechanics. The fuzzy gain scheduler parameters were computed offline and the simulation was run until the swing foot touched the ground plane to complete a single step. A simulation step time of t = 0.003 was used. Two example simulations are shown. One with white noise and no external disturbances, another with white noise and a single 6 Nm torque impulse on the swing leg at 4 seconds into the gait. In both cases the white noise at joint θ_1 was set to $\pm 1.15\ deg$ which replicated the noise in the inertial measurement unit. The white noise at

joints θ_2, θ_3, and θ_4 was $\pm$ 0.12 deg which replicated the accuracy of the encoders in the motors. Finally commanded joint torques where limited to $\pm$ 20 Nm to corresponding to the maximum continuous torques of the motors on the actual platform.

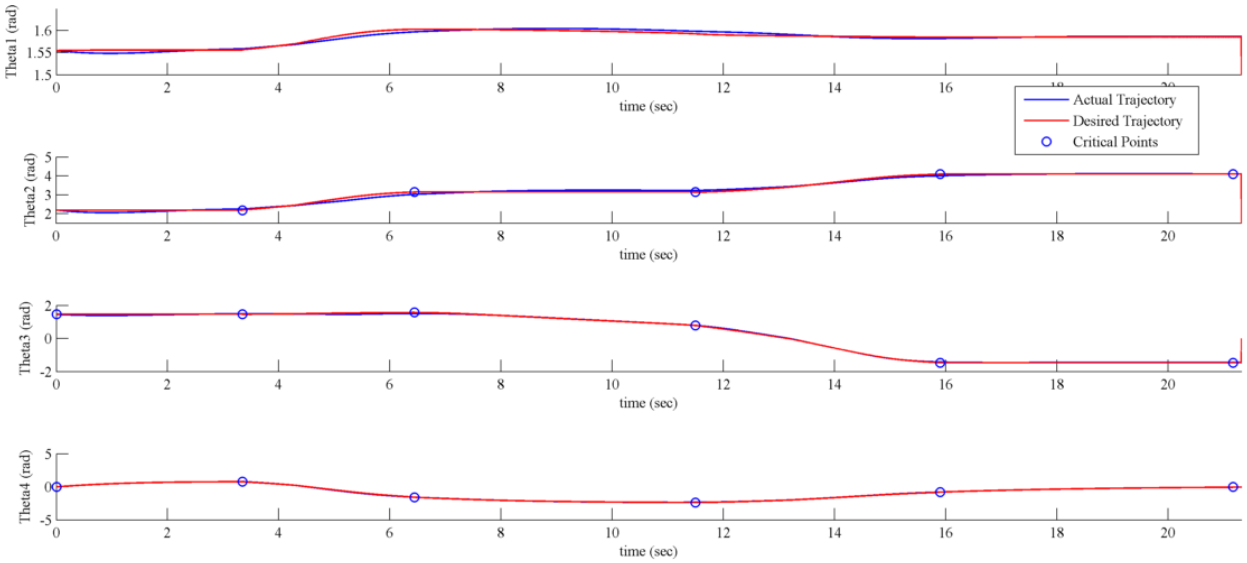

Fig. 80 Unperturbed System with White Noise, Full Trajectory Shown

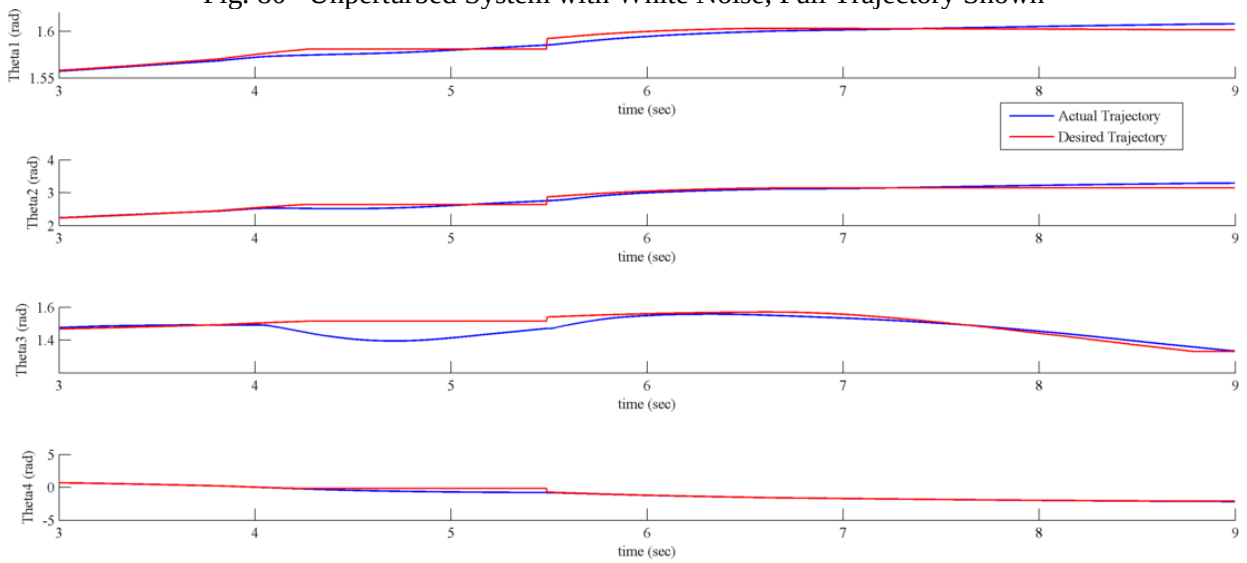

Fig. 81 Perturbed System (6 Nm Impulse on Joint 1 at 4 seconds) with White Noise, Partial Trajectory Shown During System Recovery

6 CONCLUSIONS

The goal of this project was to use a specific set of actuators to build the tallest tri-pedal robot possible capable of taking multiple successive steps. A robust and light weight hardware platform was created that when standing erect is over 10ft tall. Due to actuator reliability and availability the strict initial goals of this project were impossible to complete. Therefore the scope of the project was altered to include the development of a robust balance controller for a three-legged under-actuated robotic platform. This modified project scope was completed. A series of linear controllers were created about a set of quasi-statically stable equilibrium points where if strung together form a gate in which swing foot ground clearance is adequate and swing foot placement is accurate and soft. This step was completed in simulation in less than 25 seconds with continuous white noise and a single external impulse disturbance.

7 NEXT STEPS

The next steps for this project are to obtain a new set of actuators and reassemble the robot. Once this is completed testing could continue on either the swing through gait method or the balanced gait method. The software is already in place for continuing the swing through gait testing. The current balance controller is only implemented in Matlab. It would have to be adapted to the onboard Linux framework for the robot but considering the algorithms behind the controller are very simple the implementation should be quite straight forward. In addition once a single robust step is developed multistep testing can commence. At this point the single stance leg hip lockouts could be removed and multi-lockout adapter will have to be developed. This system would have to be able to actuate a lockout assembly to affix the hip yaw orientations as desired to take a step in a particular direction.

REFERENCES

[1] J. R. Heaston, *Design of a Novel Tripedal Locomotion Robot and*, Blacksburg, 2006.

[2] D. H. D. L. P. R. Ivette Morazzani, "Novel Tripedal Mobile Robot and Considerations for Gait Planning Strategies Based on Kinematics," in *Recent Progress in Robotics: Viable Robotic Services to Human*, Springer Berlin Heidelberg, 2008, pp. 35-48.

[3] D. W. H. Jeremy R. Heaston, "Design Optimization of a Novel Tripedal Locomotion Robot Through Simulation and Experiments for a Single Step Dynamic Gait," in *ASME 2007 International Design Engineering Technical Conferences*, Las Vegas, 2007.

[4] I. Morazzani, *Investigation of Standing Up Strategies and Considerations for Gait*, Blacksburg, 2008.

[5] D. H. Ping Ren, "Instantaneous Kinematics and Singularity Analysis of a Novel Three-Legged Mobile Robot with Active S-R-R-R Legs," in *ASME 2008 International Design Engineering Technical Conferences*, New York, 2008.

[6] I. M. D. H. Ping Ren, "Forward and Inverse Displacement Analysis of a Novel Three-Legged Mobile Robot Based on the Kinematics of In-Parallel Manipulators," in *ASME 2007 Internation Design Engineering Technical Conference*, Las Vegas, 2007.

[7] P. Ren, *Kinematics Analysis of Two Parallel Locomotion Mechanisms*, Blacksburg, 2010.

[8] K. J. A. M. W. S. Daniel J. Block, The ReactionWheel Pendulum, Urbana-Champaign: Morgan & Claypool, 2007.

[9] Z. H. a. H. D. Fangzheng Xue, "Balance Control for an Acrobot," in *Chinese Control and Decision Conference (CCDC)*, Beijing, 2011.

[10] K. M. P. Scott C. Brown, "Intelligent Control for an Acrobot," *Journal of Intelligent and Robotic Systems*, vol. 18, no. 18, pp. 209-248, 1997.

[11] J. H. Richard M. Murray, "A Case Study in Approximate Linearization:," Electronics Research Laboratory, University of California Berkeley, Berkely, 1991.

[12] K. Ogata, System Dynamics, Upper Saddle River: Pearson Education Inc., 2004.

[13] D. A. L. Robert L. Williams, Linear State-Space Control Systems, Hoboken: John Wiley & Sons Inc., 2007.

[14] W. S. H. V. B. J. S. Bart Paijmans, "A gain-scheduling control technique for mechatronic systems with position dependent dynamics," in *American Control Conference*, Minneapolis, 2006.

[15] W. J. R. Daniel J. Stilwell, "Interpolation Methods for Gain Scheduling," in *Conference on Decision and Control*, Tampa, 1998.

[16] W. J. R. Daniel J. Stilwell, "Interpolation of observer state feedback controllers for gain scheduling,"

IEEE Transactions on Automatic Control, vol. 44, no. 6, pp. 1225-1229, 1999.

[17] E. C. Fabio Previdi, "Design of a Gain Scheduling Controller for Knee-Joint Angle Control by Using Functional Electrical Stimulation," *IEEE Transactions on Control Systems Technology,* vol. 11, no. 3, pp. 310-324, 2003.

[18] H. H. H. Schulte, "Fuzzy state feedback gain scheduling control of servo-pneumatic actuators," *Control Engineering Practice,* vol. 12, no. 5, pp. 639-650, 2004.

[19] S. E. K.U. Klatt, "Gain-scheduling trajectory control of a continuous stirred tank reactor," *Computers and Chemical Engineering,* vol. 22, no. 4/5, pp. 491-502, 1998.

[20] H. J. N. B. B. Khalil Jouili, "An advanced fuzzy logic gain scheduling trajectory control for nonlinear systems," *Journal of Process Control,* vol. 20, no. 1, pp. 426-440, 2010.

[21] J. S. S. Wilson J. Rugh, "Research on Gain Scheduling," *Automatica,* vol. 36, no. 10, pp. 1401-1425, 2000.

[22] W. J. Rugh, "Analytical Framework for Gain Scheduling," *Control Systems,* vol. 11, no. 1, pp. 79-84, 1991.

[23] A. M. P. P. P. K. E. E. C. Isaac Kaminer, "A Velocity Algorithm for the Implementation of Gain-Scheduled Controllers," *Automatica,* vol. 31, no. 8, pp. 1185-1191, 1995.

APPENDIX

APPENDIX A – SHAFT STRESS CALCULATIONS

$$stress = \tau = \tau_{Torsion} + \tau_{Bending} = \frac{2T}{\pi r^3} + \frac{M}{\pi r^3}$$

Where "T" is the torque about the shaft axis and "M" is the bending moment on the shaft with no bearing support (very conservative estimate)

$$T = 14.4\ Nm\ x\ 3.0\ Factor\ of\ Safety = \ 43.2\ Nm$$

$$M = 29.5\ Nm\ x\ 3\ Factor\ of\ Safety = 88.5\ Nm$$

$$r = \frac{1}{4} inch = 0.00635\ m$$

$$\therefore \quad \tau = 217.4\ MPa$$

Shear Strength of 6061 Aluminum = 207 MPa

APPENDIX B – SHAFT KEYWAY STRESS CALCULATIONS

$$Torque = T = Force\ x\ Radius = Fr$$

$$\therefore \quad F = \frac{T}{r} = \frac{14.4\ Nm\ x\ 3}{0.00635\ m} = 6{,}803\ N$$

$$stress = \ \tau = \ \frac{Force}{Area} = \frac{F}{A} = \frac{6{,}803\ N}{0.0381\ m^2} = 0.178\ MPa = negligable$$